AD-A074 608 NAVAL WEAPONS CENTER CHINA LAKE CA F/G 16/4.1
AERODYNAMIC COEFFICIENTS FOR THE SIX-INCH TVC (TVC6) MISSILE.(U)
JUN 78 W H CLARK
UNCLASSIFIED NWC-TM-3404 GIDEP-E128-0976 NL

| OF |
AD
A074608

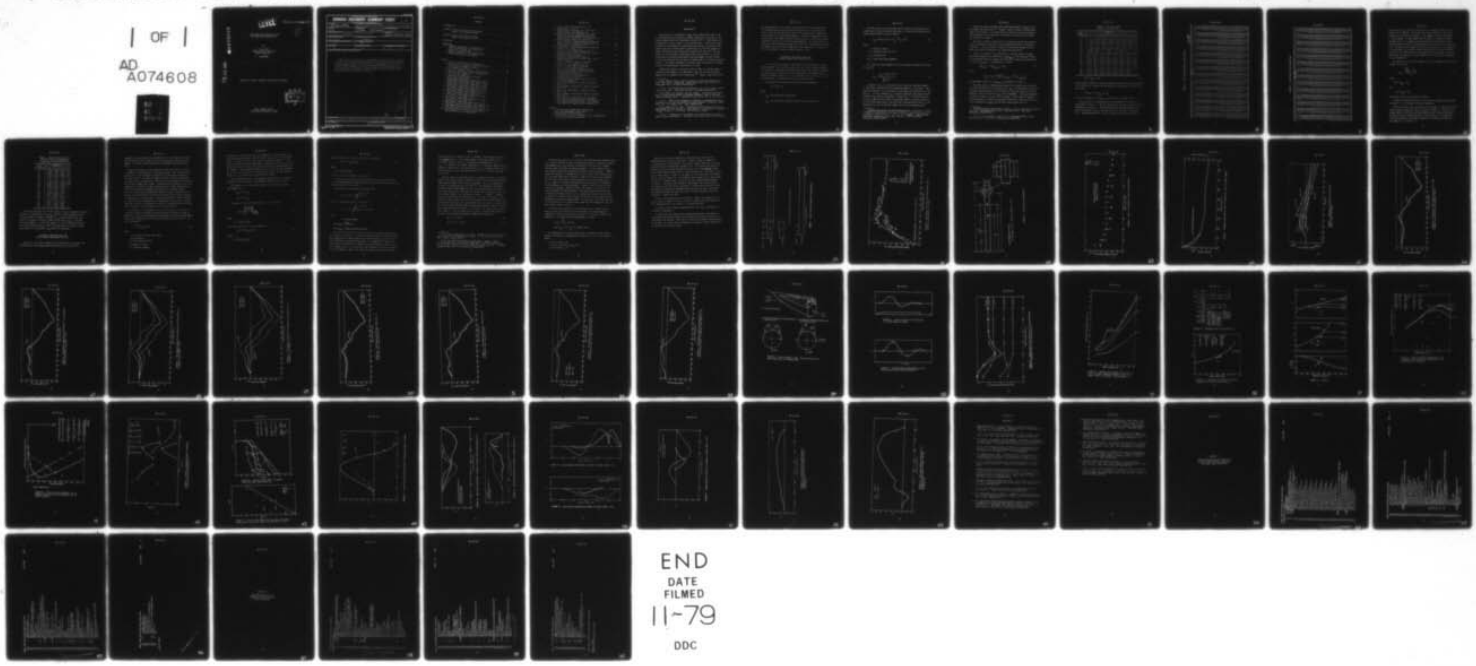

END
DATE
FILMED
11-79
DDC

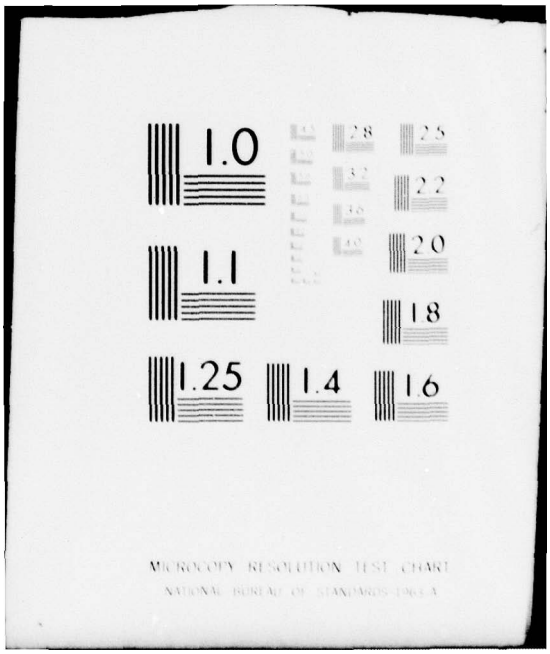
1.0
1.1
1.25
1.4
1.6
2.8
3.2
3.6
4.0
2.5
2.2
2.0
1.8
MICROCOPY RESOLUTION TEST CHART
NATIONAL BUREAU OF STANDARDS 1963-A

NWC Technical Memorandum 3404

AERODYNAMIC COEFFICIENTS FOR THE SIX-INCH TVC (TVC6) MISSILE

by

W.H. Clark
Weapon Synthesis Division
Weapons Department

June 1978

Approved for public release; distribution unlimited.

NAVAL WEAPONS CENTER
China Lake, California 93555

29 NOV 1978

OMB NO. 22-R0336

GOVERNMENT-INDUSTRY DATA EXCHANGE PROGRAM

GENERAL DOCUMENT SUMMARY SHEET

1 OF 1

Please Type All Information – See Instructions on Reverse

1. ACCESS NUMBER: E128-0976	2. COMPONENT/PART NAME PER GIDEP SUBJECT THESAURUS: General Technical Data, Problems of Hardware in Environments	
3. APPLICATION: Missile	4. MFR NOTIFICATION: [ ] NOTIFIED [X] NOT APPLICABLE	5. DOCUMENT ISSUE (Month/Year): June 1978
6. ORIGINATOR'S DOCUMENT TITLE: Aerodynamic Coefficients for the Six-Inch TVC (TVC6) Missile		7. DOCUMENT TYPE: [X] GEN RPT [ ] NONSTD PART [ ] SPEC
8. ORIGINATOR'S DOCUMENT NUMBER: NWC TM 3404	9. ORIGINATOR'S PART NAME/IDENTIFICATION: TVC6 Missile	
10. DOCUMENT (SUPERSEDES) (SUPPLEMENTS) ACCESS NO.: None	11. ENVIRONMENTAL EXPOSURE CODES: N/A	
12. MANUFACTURER: N/A	13. MANUFACTURER PART NUMBER: N/A	14. INDUSTRY/GOVERNMENT STANDARD NUMBER: N/A

15. OUTLINE, TABLE OF CONTENTS, SUMMARY, OR EQUIVALENT DESCRIPTION

This report is a final report documenting the predictions of the static aerodynamic coefficients (normal and side force and pitch and yaw moments) used in computer simulations of the Navy's 6-inch-diameter thrust vector controlled ASRAAM candidate. Although the predictions described are for a specific missile configuration, the techniques used are sufficiently general to be applicable to a variety of slender bodies of revolution that are expected to fly at high angles of attack.

16. KEY WORDS FOR INDEXING: Static Aerodynamic Coefficients; Advanced Short-Range Air-to-Air Missile; Computer Simulation; Computer Programs; Force & Pitching Moment Coefficients (Doc Des--P)

17. GIDEP REPRESENTATIVE: M. H. Sloan	18. PARTICIPANT ACTIVITY AND CODE: Naval Weapons Center, China Lake, CA (X7)

DD FORM 1 NOV 79 2000

CONTENTS

Tables:

4

INTRODUCTION

The validity of the subsonic normal force coefficients used in the air intercept missile evaluation (AIMVAL) simulation of the Navy's "D" concept missile was first questioned in April 1977.[1] (This missile will be referred to in this report as the TVC6 missile.) Errors were found to exist in the aerodynamic coefficients and action to recalculate the normal force and pitching moment coefficients for TVC6 was suggested.[2] These coefficients were recalculated during fiscal year 1977; the new values of the aerodynamic coefficients have been included in the simulation models currently being used by NWC and Hughes Aircraft Company in the short-range air-to-air missile (SRAAM) generic airframe evaluation efforts. This report documents the methods used to estimate the normal force and pitching moment coefficients for TVC6.

Symmetrical bodies of revolution such as TVC6, at certain angles of attack and Mach numbers, can experience large side forces and yawing moments due to asymmetric flow separation.[3-6] Indeed, these side forces

---

[1] Naval Weapons Center. Need for Review of Simulation Employed at ACM(I) (U), by W.F. Cartwright. China Lake, Calif., NWC 20 April 1977. (Reg. Memo 015/14, document UNCLASSIFIED.)

[2] ———. 6" TVC Normal Force Coefficient (U), by W.H. Clark. China Lake, Calif., NWC. (Reg. Memo 3914-93-77, document UNCLASSIFIED.)

[3] W.H. Clark, J.R. Peoples, and M.M. Briggs. "Occurrence and Inhibition of Large Yawing Moments During High-Incidence Flight of Slender Missile Configurations," *J. Spacecraft and Rockets*, Vol. 10, No. 8 (1973).

[4] ———. "Body Vortex Formation on Missiles in Incompressible Flow," presented at the AIAA 4th Atmospheric Flight Mechanics Conference, Hollywood, Fla., 8-10 August 1977. Paper UNCLASSIFIED.

[5] P.J. Lamont and B.L. Hunt. "Pressure and Force Distributions on a Sharp-Nosed Circular Cylinder at Large Angles of Inclination to a Uniform, Subsonic Stream," *J. Fluid Mech.*, Vol 76, Part 3 (1976).

[6] ———. "Prediction of Aerodynamic Out-of-Plane Forces on Ogive-Nosed Circular Cylinders," *J. Spacecraft and Rockets*, Vol. 14, No.1 (1977).

5

and yawing moments, which tend to move the missile body perpendicular to the plane containing the missile axis and the free stream velocity vector, for some configurations can be of the same order of magnitude as the normal force and pitching moment. A realistic evaluation of the TVC6 missile's performance should include a study of sensitivity in performance to these side forces and yawing moments. For this reason, efforts also were undertaken during fiscal year 1977 to estimate the forces and moments associated with asymmetrical flow separation for inclusion in the six degree-of-freedom computer models of TVC6.

ESTIMATE OF THE NORMAL FORCE AND PITCHING MOMENT COEFFICIENTS FOR TVC6

In arriving at the values of the normal force coefficient (C_N) and pitching moment coefficient (C_M) given in this report, maximum possible use was made of existing Agile wind tunnel data. The problem in scaling the coefficients from Agile to TVC6 is that Agile was designed with a length-to-diameter ratio (ℓ/d) of 12.5 and the ratio for TVC6 ℓ/d is 20. The method used to perform the scaling is outlined below.

The normal force coefficient for TVC6 can be expressed as

$$C_N = C_{N_B} + C_{N_F} \tag{1}$$

where

C_{N_B} = the body alone coefficient

C_{N_F} = the effective contribution due to the six tail fins.

The body alone force coefficient can be scaled from the Agile wind tunnel data by using the method described in a National Aeronautics and Space Administration technical report.[7]

$$C_{N_B} = \sin 2\alpha \cos\alpha/2 + \eta C_{D_c} A_p/A_r \sin^2\alpha \qquad (2)$$

where

α = angle of attack

A_r = reference area ($\equiv \Pi d^2/4$)

A_p = planform area

ηC_{D_c} = cross flow drag parameter.

The cross flow drag parameter can be determined from measured values of C_{N_B} from

$$\eta C_{D_c} = \frac{C_{N_B} - \sin 2\alpha \cos\alpha/2}{\frac{A_p}{A_r} \sin^2\alpha} \qquad (3)$$

In general, ηC_{D_c} is a function of both the cross flow Mach number, M_c ($\equiv M_\infty \sin\alpha$), and the cross flow Reynolds number, R_x ($\equiv R_\infty \sin\alpha$). (However, see Footnote 4 for a discussion concerning the correlation of ηC_{D_c} with R_x.) For our purposes, R_x is usually large and only supercritical values of ηC_{D_c} need be considered. Because ηC_{D_c} is a "weak" function of R_x for supercritical values of Reynolds number, and because there is not sufficient Agile data to perform useful extrapolations with R_x, the dependence of ηC_{D_c} on Reynolds number will not be considered here.

---

[7] National Aeronautics and Space Administration. *Prediction of Static Aerodynamic Characteristics for Space - Shuttle - Like and Other Bodies at Angles of Attack From 0° to 180°*, by L.H. Jorgensen. Ames Research Laboratory, Sunnyvale, Calif. NASA, Jan 1973. (NASA TN-D-6996, publication UNCLASSIFIED.)

Contractor reports provide wind tunnel measurements of C_{N_B} for several Agile configurations.[8,9] (Figure 1 shows the Agile configurations used in this study.) From these data the value of ηC_{D_c} was calculated (from Equation 3) and plotted as a function of cross flow Mach number, M_c, as shown in Figure 2.

The data of Figure 2 shows that ηC_{D_c} versus M_c follows two distinct curves, depending on whether the free stream Mach number is subsonic or supersonic. The solid lines in Figure 2 were faired through the data points and used to compute the C_N values described below.

Given the values for ηC_{D_c} from Figure 2 and the values for Agile body alone normal force coefficient, $(C_{N_B})_{Agile}$, from Footnotes 8 and 9 it is straightforward to compute the body alone normal force coefficient for TVC6, $(C_{N_B})_{TVC6}$. From Equation 2 we have

$$(C_{N_B})_{TVC6} = (C_{N_B})_{Agile} + \Delta C_{N_B} \tag{4}$$

where

$$\Delta C_{N_B} = \eta C_{D_c} \sin^2\alpha \left((A_p/A_r)_{TVC6} - (A_p/A_r)_{Agile} \right)$$

The estimated values for $(C_{N_B})_{TVC6}$ are tabulated in Table 1.

The final step in computing the normal force coefficient for TVC6 is to obtain the effective fin normal force, C_{N_F}. The appropriate values for C_{N_F} were obtained directly from Footnote 8, using the values of the configuration that utilized the "C_{62F}" fin arrangement. (This configuration is shown in Figure 1 at the top of the page.) The values for C_{N_F} were obtained simply by taking the difference between the values of C_N for the full configuration ($C_{N_{B+F}}$) and the body alone values; that is,

---

[8] McDonnell Douglas Astronautics Co.-West. *Agile Configuration Development Test.* Huntington Beach, Calif., MDC, April 1974. (MDC G51J6 publication UNCLASSIFIED.)

[9] ———. *Agile External Geometry Test.* Huntington Beach, Calif., MDC, June 1973. (MDC G4027, publication UNCLASSIFIED.)

TABLE 1. TVC6 Body Alone
Normal Force Coefficient.

Angle of attack	Mach no.							
	0.6	0.8	0.95	1.1	1.2	1.6	2.0	3.0
0	0	0	0	0	0	0	0	0
5	0.22	0.33	0.32	0.32	0.24	0.39	0.24	0.36
10	0.74	0.85	0.87	0.89	0.79	0.95	0.99	1.29
15	1.36	1.74	1.69	1.87	1.79	2.31	2.66	3.0
20	2.46	3.04	3.76	3.46	3.54	4.66	5.01	5.17
25	4.06	4.89	5.11	5.73	6.16	7.76	7.89	7.34
30	6.09	6.96	7.52	9.07	9.45	11.23	10.7	9.63
35	8.49	9.21	...	12.8	...	14.8	...	...
40	11.0	11.6	13.2	16.6	16.8	17.7	16.0	14.6
45	13.22	14.3	16.2	20.5	20.4	20.5	18.6	17.1
50	15.1	17.2	19.3	24.3	23.6	23.2	21.3	19.5
55	16.5	20.1	22.3	27.5	26.4	25.8	23.8	22.0
60	18.8	22.7	24.3	29.9	28.8	28.6	26.3	24.3
65	20.4	25.4	25.8	31.9	31.0	31.1	28.6	26.4
70	23.1	26.9	27.1	33.5	33.4	33.0	30.5	28.3
75	24.9	28.4	28.2	35.3	35.6	34.2	32.0	29.9
80	26.2	28.9	29.4	37.6	37.4	35.3	33.2	...
85	27.1	29.1	30.3	39.0	38.4	36.0	33.9	...
90	26.9	29.4	31.3	39.2	38.5	36.4	34.3	...

$$C_{N_F} = C_{N_{B+F}} - C_{N_B} \tag{5}$$

By scaling the values for C_{N_F} thus obtained from the 8-inch Agile diameter to the 6-inch TVC6 diameter we can simply add the values of C_{N_F} and C_{N_B}, as follows:

$$(C_N)_{TVC6} = (C_{N_B})_{TVC6} + C_{N_F} \tag{6}$$

The final estimates for $(C_N)_{TVC6}$ are tabulated in Tables 2 and 3.

The procedure for estimating the pitching moment coefficient is illustrated in Figure 3. As this figure shows, we require two additional parameters to obtain C_M. These parameters are the body normal force center of pressure, $\bar{X}_{cp_B}/\ell$, and the effective fin center of pressure, $\bar{X}/C_r$. These parameters also can be obtained from Footnotes 8 and 9.

TABLE 2. TVC6 Pitching Moment Coefficients.

A_T = 0.1963
X_T = 58.31

	Mach no.												
α	0	0.4	0.6	0.8	0.9	1.1	1.2	1.4	1.6	1.8	2.0	2.2	3.0
0.000	0.000	0.000	0.000	0.000	0.000	0.000	0.000	0.000	0.000	0.000	0.000	0.000	0.000
5.000	-0.310	-0.310	-0.310	0.210	0.070	0.010	-0.350	0.010	0.390	0.100	-0.120	-0.310	0.450
10.000	-0.990	-0.990	-0.990	-0.630	-0.630	-0.000	-0.950	-0.760	-0.310	-0.330	-0.030	0.170	0.950
15.000	-1.780	-1.780	-1.780	-0.620	-0.910	-0.490	-0.750	-0.190	0.410	1.260	2.150	2.320	3.000
20.000	-2.040	-2.040	-2.040	-1.070	-0.000	-0.520	-0.150	1.440	3.100	4.350	5.560	5.620	5.850
25.000	-4.240	-4.240	-4.240	-2.690	-2.030	-1.310	-0.070	2.350	4.730	5.590	6.220	6.050	5.390
30.000	-4.190	-4.190	-4.190	-3.130	-2.550	-0.100	1.010	3.480	5.070	5.930	5.980	5.720	4.680
35.000	-4.910	-4.910	-4.910	-4.250	-3.330	-0.700	0.350	2.930	5.090	6.030	5.810	5.000	2.800
40.000	-5.910	-5.910	-5.910	-5.420	-1.670	2.070	3.370	4.580	5.770	6.940	6.100	5.870	2.960
45.000	-5.610	-5.610	-5.610	-5.040	-0.040	3.160	5.140	5.370	5.020	6.990	6.370	6.160	3.490
50.000	-2.070	-2.070	-2.070	-0.500	2.010	5.950	5.150	7.410	8.050	8.690	8.310	8.050	5.020
55.000	-0.200	-0.200	-0.200	2.350	3.950	7.340	8.560	9.520	8.120	8.130	8.110	7.850	5.810
60.000	2.720	2.720	2.720	5.440	5.910	9.960	9.490	10.040	10.060	10.010	9.390	9.100	7.990
65.000	1.070	1.070	1.070	3.000	3.490	8.220	8.970	8.490	7.120	8.470	8.830	8.810	6.690
70.000	-3.570	-3.570	-3.570	-2.740	-3.750	-3.900	-3.550	-2.650	-1.500	-1.930	-2.330	-2.630	-2.810
75.000	-5.100	-5.100	-5.100	-2.740	-4.770	-7.330	-5.750	-5.820	-6.060	-5.030	-5.200	-5.250	-5.450
80.000	-8.440	-8.440	-8.440	-8.000	-9.750	-11.700	-11.790	-11.490	-11.280	-11.530	-11.700	-11.650	-11.440
85.000	-14.530	-14.530	-12.530	-12.670	-13.070	-14.790	-14.660	-14.400	-14.150	-14.670	-15.150	-15.010	-14.440
90.000	-14.180	-14.180	-14.180	-14.870	-16.210	-20.550	-17.060	-15.590	-17.260	-18.030	-18.650	-18.410	-17.440
95.000	-15.640	-15.240	-15.240	-15.600	-16.060	-16.090	-13.300	-15.120	-17.750	-15.170	-18.560	-18.320	-17.440
100.000	-16.920	-16.920	-16.920	-20.220	-21.440	-20.820	-25.060	-25.030	-25.400	-25.200	-24.950	-24.670	-23.440
105.000	-25.060	-25.060	-25.060	-25.400	-27.360	-35.570	-33.260	-33.740	-32.620	-31.510	-30.800	-30.520	-29.370
110.000	-28.070	-28.070	-28.070	-29.640	-30.780	-37.400	-35.950	-35.850	-34.500	-33.690	-32.830	-32.490	-31.110
115.000	-31.570	-31.570	-31.570	-32.960	-37.770	-44.020	-43.630	-43.190	-42.040	-41.290	-39.930	-39.650	-37.550
120.000	-34.500	-34.500	-34.500	-39.500	-41.150	-49.240	-47.560	-46.790	-45.970	-44.350	-42.700	-42.190	-40.130
125.000	-35.260	-35.260	-35.260	-37.070	-39.190	-45.060	-44.260	-43.880	-43.480	-41.670	-39.690	-39.030	-37.190
130.000	-32.270	-32.270	-32.270	-34.960	-35.190	-39.650	-39.050	-39.390	-39.750	-38.020	-36.290	-35.830	-33.990
135.000	-30.250	-30.250	-30.250	-31.040	-31.980	-35.060	-35.060	-35.530	-35.360	-34.110	-32.830	-32.440	-30.910
140.000	-26.110	-26.110	-26.110	-26.940	-27.740	-33.050	-33.810	-33.480	-33.170	-32.130	-31.100	-30.710	-29.150
145.000	-25.290	-25.290	-25.290	-26.350	-27.580	-31.460	-31.090	-30.550	-29.830	-29.090	-28.110	-27.790	-26.490
150.000	-22.460	-22.460	-22.460	-24.010	-24.550	-27.370	-27.340	-27.540	-27.820	-26.950	-25.180	-25.740	-24.210
155.000	-18.880	-18.880	-18.880	-20.570	-20.760	-21.940	-22.250	-22.670	-23.010	-22.530	-22.180	-21.950	-21.040
160.000	-14.150	-14.150	-14.150	-15.650	-16.770	-16.440	-15.440	-17.420	-16.330	-17.990	-17.490	-17.570	-17.900
165.000	-9.070	-9.070	-9.070	-10.910	-10.000	-11.340	-11.160	-12.000	-12.980	-13.170	-13.280	-13.500	-14.400
170.000	-6.720	-6.720	-6.720	-7.210	-7.520	-7.470	-7.070	-7.470	-7.960	-7.910	-7.690	-7.960	-9.040
175.000	-2.600	-2.600	-2.600	-3.520	-3.570	-3.510	-3.070	-3.550	-4.020	-3.450	-2.830	-2.990	-3.620
180.000	0.000	0.000	0.000	0.000	0.000	0.000	0.000	0.000	0.000	0.000	0.000	0.000	0.000

TABLE 3. TVC6 Normal Force Coefficient.

	Mach number												
α	0.600	0.400	0.600	0.800	0.900	1.100	1.200	1.400	1.600	1.800	2.000	2.200	3.000
0.000	0.000	0.000	0.000	0.000	0.000	0.000	0.000	0.000	0.000	0.000	0.000	0.000	0.000
5.000	0.320	0.320	0.320	0.430	0.440	0.470	0.390	0.460	0.540	0.440	0.340	0.360	0.460
10.000	1.090	1.090	1.090	1.200	1.230	1.290	1.200	1.300	1.400	1.370	1.340	1.400	1.640
15.000	1.860	1.860	1.860	2.240	2.210	2.370	2.310	2.610	2.910	3.010	3.110	3.180	3.450
20.000	3.260	3.260	3.260	3.840	4.320	4.260	4.300	4.780	5.260	5.330	5.510	5.540	5.670
25.000	5.160	5.160	5.160	5.990	6.140	6.830	7.180	7.820	8.460	8.530	8.560	8.430	7.990
30.000	7.390	7.390	7.390	8.260	8.600	10.270	10.590	11.360	12.130	11.840	11.550	11.340	10.480
35.000	9.990	9.990	9.990	10.710	11.400	14.200	14.380	14.990	15.600	14.970	14.350	14.130	13.250
40.000	12.400	12.400	12.400	13.000	14.000	17.860	18.060	18.380	18.700	17.850	17.000	16.720	15.600
45.000	14.620	14.620	14.620	15.700	16.870	21.600	21.480	21.490	21.500	20.550	19.600	19.300	18.100
50.000	16.400	16.400	16.400	18.500	19.800	25.300	24.620	24.460	24.300	23.300	22.300	21.940	20.500
55.000	17.700	17.700	17.700	21.300	22.770	28.700	27.580	27.240	26.900	25.850	24.800	24.440	23.000
60.000	19.900	19.900	19.900	23.800	24.970	31.300	30.140	29.920	29.700	28.550	27.300	26.900	25.300
65.000	21.300	21.300	21.300	26.300	26.700	33.200	32.240	32.170	32.100	30.850	29.600	29.160	27.400
70.000	24.000	24.000	24.000	27.800	28.100	34.900	34.700	34.300	33.900	32.700	31.500	31.060	29.300
75.000	25.500	25.500	25.500	29.000	29.100	36.600	35.840	36.020	35.200	34.100	33.000	32.580	30.900
80.000	26.700	26.700	26.700	29.400	29.870	36.500	36.300	37.250	36.200	35.200	34.200	33.560	31.000
85.000	27.900	27.900	27.900	29.900	30.700	39.800	39.200	38.000	36.800	35.850	34.900	34.120	31.600
90.000	27.600	27.600	27.600	30.100	31.470	40.200	39.440	38.270	37.100	36.200	35.300	34.440	31.000
95.000	27.900	27.900	27.900	29.900	30.700	39.800	39.200	38.000	36.800	35.850	34.900	34.120	31.000
100.000	26.700	26.700	26.700	29.400	29.870	36.500	36.300	37.250	36.200	35.200	34.200	33.560	31.000
105.000	25.500	25.500	25.500	29.000	29.100	36.600	35.840	36.020	35.200	34.100	33.000	32.580	30.900
110.000	24.000	24.000	24.000	27.800	28.100	34.900	34.700	34.300	33.900	32.700	31.500	31.060	29.300
115.000	21.300	21.300	21.300	26.300	26.700	33.200	32.240	32.170	32.100	30.850	29.600	29.160	27.400
120.000	19.900	19.900	19.900	23.800	24.970	31.300	30.140	29.920	29.700	28.550	27.300	26.900	25.300
125.000	17.700	17.700	17.700	21.300	22.770	28.700	27.580	27.240	26.900	25.850	24.800	24.440	23.000
130.000	16.400	16.400	16.400	18.500	19.800	25.300	24.620	24.460	24.300	23.300	22.300	21.940	20.500
135.000	14.620	14.620	14.620	15.700	16.870	21.600	21.480	21.490	21.500	20.550	19.600	19.300	18.100
140.000	12.400	12.400	12.400	13.000	14.000	17.860	18.060	18.380	18.700	17.850	17.000	16.720	15.600
145.000	9.990	9.990	9.990	10.710	11.400	14.200	14.380	14.990	15.600	14.970	14.350	14.130	13.250
150.000	7.390	7.390	7.390	8.260	8.600	10.270	10.590	11.360	12.130	11.840	11.550	11.340	10.480
155.000	5.160	5.160	5.160	5.990	6.140	6.830	7.180	7.820	8.460	8.530	8.560	8.430	7.990
160.000	3.260	3.260	3.260	3.840	4.320	4.260	4.300	4.780	5.260	5.330	5.510	5.540	5.670
165.000	1.860	1.860	1.860	2.240	2.210	2.370	2.310	2.610	2.910	3.010	3.110	3.180	3.450
170.000	1.090	1.090	1.090	1.200	1.230	1.290	1.200	1.300	1.400	1.370	1.340	1.400	1.640
175.000	0.320	0.320	0.320	0.430	0.440	0.470	0.390	0.460	0.540	0.440	0.340	0.360	0.460
180.000	0.000	0.000	0.000	0.000	0.000	0.000	0.000	0.000	0.000	0.000	0.000	0.000	0.000

The values for X_{cp}/ℓ are shown in Figure 4 for angles of attack in the region 0 to 90 degrees. The solid curve shown in Figure 5 was faired through the data points of Figure 4. For angles of attack, 90 degrees $\leq \alpha \leq 160$ degrees, it was assumed that the center of pressure followed the same curve. For angles of attack approaching 180 degrees it was assumed that the center of pressure moved to the blunt end at the nozzle exit. Although this assumption is arbitrary and certain to be complicated by the presence of the rocket plume further efforts were not considered justified. The TVC6 missile is not expected to fly at angles of attack approaching 180 degrees, and performance studies will not be compromised by this assumption.

The effective fin center of pressure, $\bar{X}/C_r$, is obtained from Footnote 8 through the relation

$$\bar{X}/C_r = \frac{\frac{-\Delta C_M}{\Delta C_N} d - \ell_{FLE}}{C_r} \tag{7}$$

where

$$\Delta C_M = C_{M_{B+F}} - C_{M_B}$$

and

$$\Delta C_N = C_{N_{B+F}} - C_{N_B}$$

The values of $\bar{X}/C_r$ are tabulated in Table 4.

A computer program was written to perform the computations indicated in Figure 3. This program is given in Appendix A.

The fin location, X_{FLE}, was varied in an attempt to "match" the Agile static stability margin at launch, as shown in Figure 6. Although the present model for the TVC6 pitching moment estimate does not duplicate the Agile stability margin exactly, a value of $X_{FLE} = 110$ inches was selected as giving a reasonable compromise over launch Mach numbers in the range of $0.7 \leq$ Mach ≤ 1.2.

TABLE 4. Effective Fin Center of Pressure, X/C_r, Configuration $B_6\ N_{21}\ C_{62F}\ A_9$ (See Footnote 8).

Angle of attack	Mach no.			
	0.8	1.1	1.6	2.0
0	6.52	1.86	1.42	5.2
5	6.52	1.86	1.42	5.2
10	1.48	0.19	-0.81	0.91
15	2.39	2.39	0.52	2.0
20	1.52	1.02	2.52	0.66
25	1.13	0.65	1.57	0.32
30	0.42	0.97	0.08	-0.42
35	-0.19	0.43	1.69	-0.81
40	0.81	0.64	0.13	...
45	1.19	0.16	0.66	...
50	1.76	-0.14	0.65	...
55	1.97	0.08	1.13	...
60	1.13	-1.09	-0.2	...
65	2.6	-0.91	0.52	...
70	1.27	-0.81	1.41	...
75	2.08	0.32	0.39	...
80	5.32	1.41	0.96	...
85	1.19	1.36	1.19	...
90	1.1	1.19	1.86	...

The final estimates for the TVC6 values of C_M are tabulated in Table 2. Finally, the sensitivity to C_N, X_{cp}, and $\bar{X}/C_r$ of the estimated values of C_M are shown in Figures 7 through 14. As these figures show, the center of pressure of the body alone normal force, X_{cp_B}, is the most critical parameter. If the TVC6 missile is to be considered seriously as a future SRAAM candidate, then a thorough study of missile overall performance to the parameter X_{cp_B} should be undertaken.

ESTIMATE OF THE SIDE FORCE AND YAWING MOMENT COEFFICIENTS FOR TVC6

This part of the report summarizes the method used to estimate the TVC6 side force and yawing moment coefficients that arise due to

asymmetric flow separation on the missile body. The reader is advised that the method used is based on an (as yet) unproven, semi-empirical method. The results should be used for preliminary planning purposes only.

Figure 15 defines the "out-of-plane" or side force that occurs due to asymmetric flow separation on the missile body. The prediction technique used for the estimates is based on the information contained in Footnotes 5 and 6. The work of Lamont and Hunt is strictly applicable to conditions of incompressible, laminar flow over cylindrical afterbodies with pointed tangent ogive noses. Although these conditions are not representative of realistic flight conditions such as those experienced by TVC6, this technique nonetheless was selected for several reasons. First the flow structure observed by Lamont and Hunt is believed by the author to be qualitatively the same as that which exists under conditions of compressible, turbulent flow. Second, the method of Lamont and Hunt is simple and easily implemented for preliminary calculations. Attempts were made to correct the method for effects of compressibility and higher Reynolds numbers. These attempts will be described later.

In Footnote 5, it was shown that the "out-of-plane" or side force on the missile body was typically distributed along the body, as shown in Figure 16. This force distribution was obtained via pressure measurements around the circumference of the body at different axial locations. The force coefficient

$$C_F \equiv F / \frac{1}{2} \rho V_\infty^2 \sin^2\alpha D \qquad (8)$$

where

F = the side force per unit length

ρ = air density

V_∞ = free stream velocity

α = angle of attack

D = cylinder diameter

was shown to correlate well with the parameter $\bar{t} = X\tan\alpha/R$, where X is the axial station measured from the missile nose and R is the cylinder radius. A typical curve of C_F versus $\bar{t}$ is shown in Figure 17. This curve, with the appropriate magnitudes, completely defines the side force and distribution from which the total side force and yawing moment can be obtained. Lamont and Hunt showed that the values for the parameters $\bar{t}_A$, $\bar{t}_C$, $\bar{t}_E$, $\bar{t}_G$ correlated well with angle of attack and nose fineness ratio, $F_N \equiv L_N/D$, where L_N is the total nose length.

Also the maximum value of the parameter C_{F_B} at point B on Figure 17 was shown to be a function of the parameter $\bar{X}$, where $\bar{X} \equiv 2\ F_N \tan\alpha$.

The values of C_F at the points D and F on the curve were given approximately by

$$C_{F_D} = -0.6\ C_{F_B} \tag{9}$$

$$C_{F_F} = 0.3\ C_{F_B} \tag{10}$$

The shape of the curve from points A to C is given by

$$C_F = C_{F_B}\left(e^{\frac{\chi_B-\chi}{\tan\chi_B}}\right)\frac{\sin\chi}{\sin\chi_B} \tag{11}$$

where

$$\chi = \pi\ (\bar{t}-\bar{t}_A)/(\bar{t}_C-\bar{t}_A)$$

The curve from point C to E is defined by

$$C_F = -0.6\ C_{F_B}\ \sin\pi\xi_1 \tag{12}$$

where

$$\xi_1 = (\bar{t}-\bar{t}_C)/(\bar{t}_E-\bar{t}_C)$$

while from point E to point G the curve is defined by

$$C_F = 0.3\, C_{F_B} \sin\pi\xi_2 \tag{13}$$

where

$$\xi_2 = (\bar{t}-\bar{t}_E)/(\bar{t}_G-\bar{t}_E)$$

For $\bar{t} > \bar{t}_G$ the out-of-plane force, $C_F = 0$.

With the out-of-plane force distribution defined as outlined above it is straightforward to obtain the total side force coefficient, C_Y, and the yawing moment coefficient, C_n.

The side force coefficient is obtained from

$$C_Y = 2/\pi \sin\alpha\cos\alpha \int_0^{\bar{t} = \ell/_R \tan\alpha} C_F(\bar{t})\, d\bar{t} \tag{14}$$

and the corresponding moment coefficient is

$$C_n = 1/\pi \cos^2\alpha \int_0^{\bar{t} = \ell/_R \tan\alpha} (\bar{t}_{REF} - \bar{t})\, C_F(\bar{t})\, d\bar{t} \tag{15}$$

where

ℓ = missile length

and $t_{REF} = \frac{X_{REF}}{R} \tan\alpha$

with X_{REF} = moment reference station

The above description is a brief outline of the method discussed in more detail in Footnote 6. Using this technique Lamont and Hunt obtained good agreement with experimental data obtained under the conditions for which the theory is strictly applicable. As regards TVC6, one of the major areas of concern was to establish how the increase in missile overall fineness ratio, $\ell/_D$, would affect the magnitude of the out-of-plane forces and moments. Hence, the prediction method was applied directly

and the results of Figures 18 and 19 obtained. These figures show how the maximum side force and yawing moment coefficients depend on $\ell/_D$. The theory predicts that C_Y is essentially independent of $\ell/_D$ for $\ell/_D > 12$. However, the moment coefficient, C_n, increases rapidly with $\ell/_D$. Figure 19 shows that C_n more than doubles as $\ell/_D$ increases from 12 to 20. The reader will recall that Agile had an $\ell/_D = 12.5$ and that TVC6 had an $\ell/_D = 20$.

The next step in this analysis was to compare the theory with experimental data obtained under conditions for which both compressibility and high Reynolds number effects would be present. For these comparisons the work of Deffenbaugh was utilized.[10,11] Deffenbaugh's experiments included pressure measurements on the configurations shown in Figure 20. From these data direct comparison can be made with the generalized curve from Lamont and Hunt that was shown in Figure 17. Figure 21 compares the predicted values of the points A, B, C, E, and G of Figure 17 from Lamont and Hunt's method to those values obtained from Deffenbaugh's data. The spacing values $\bar{t}_E - \bar{t}_c$ and $\bar{t}_B$ shown on Figures 21 and 22, respectively, are in reasonable agreement with the prediction method, despite the higher Mach number and Reynolds number. The values for $\bar{t}_A$ and $\bar{t}_c$ do not agree well, however. For the prediction of C_Y and C_n for TVC6 the values for $\bar{t}_A$ and $\bar{t}_c$ for supercritical Reynolds numbers were modified to

$$\bar{t}_A = 1.0 + 0.05\alpha \tag{16}$$

$$\bar{t}_c = 9.5 + 4.7 \tan\alpha \tag{17}$$

---

[10] F.D. Deffenbaugh and W.G. Koerner. "Asymmetric Vortex Wake Development on Missiles at High Angles of Attack," *J. Spacecraft and Rockets*, Vol. 14, No. 3 (March 1977).

[11] U.S. Army Missile Research and Development Command. Summary of the 4th Meeting of the DoD/NASA High Angle of Attack Working Group, 16-17 Feb 1977. Huntsville, Ala., Redstone Arsenal, Feb 1977. (Internal Technical Note TDK-77-1, publication UNCLASSIFIED.)

With the node points (A, C, E and G) and the maximum and minimum points (B, D, and F) determined only three features remain to complete the model. The maximum value, C_{F_B}, must be corrected for the effects of compressibility, nose bluntness, and Reynolds number. To study those effects the reports referenced on Figures 22 through 26 were consulted. Figure 22 shows the variation of maximum side force, C_Y, with nose fineness ratio, F_n, for sharp-nosed ogive cylinders. Figure 23 presents some experimental data that indicates how nose bluntness affects the maximum value of C_Y. Figure 24 presents experimental data indicating the dependence of the maximum C_Y on Reynolds number. Figures 23 and 24 indicate that there is no apparent consistent trend, with respect to the effects of nose bluntness, or Reynolds number. The theoretical method does seem to bound the maximum values of C_Y for sharp-nosed bodies, as indicated in Figure 22. Figures 25 and 26 show the effects of Mach number on both maximum side force and yawing moment. In this case it is clear that the values decrease with increasing Mach number and are essentially zero for Mach numbers greater than 1.6.

In view of the above data it was decided that no attempt would be made to correct the theory for nose bluntness. The simple approach suggested in Footnote 6 was used to account for turbulent boundary layer separation. This approach was implemented as follows:

$$\text{if } R_D \equiv \frac{U_\infty D}{\upsilon} \geq 200{,}000$$

$$\text{then } C_{F_B} = 0.8\, C_{F_B}' \text{ (for laminar flow)}$$

The compressibility effects were grossly included by simply multiplying the theoretical incompressible values of C_Y and C_n by a factor, f, where

$$f = 1.0 \text{ for } M_\infty \leq 0.6$$
$$f = 1.6 - M_\infty \text{ for } 0.6 \leq M_\infty \leq 1.6$$
$$f = 0.0 \text{ for } M_\infty > 1.6$$

Next, with the method modified as described above, some further comparisons were made with other data. Figure 27 shows a comparison of the theoretical distribution of C_F along a missile body and the actual measured values of Deffenbaugh (Footnote 10). The theoretical values are higher as may be expected, because the theory is for the maximum values and the experimental values are for time-averaged data. The overall value of C_Y versus angle of attack, α, is shown for both theoretical and experimental values in Figure 28. The original theory showed the C_Y value going to zero at 70 degrees angle of attack; the data suggested approximately 50 degrees. The theory was revised to approximate this feature better and Figures 29 through 32 were obtained to compare Agile data with theory. Although the quantitative agreement with Agile data is poor, the theory does generally bound the data and, hence, could be expected to provide estimates of worst-case data.

Finally, the modified theory was used to compute the estimates of C_Y and C_n shown in Figures 33 and 34 for TVC6. These values were adjusted for compressibility by the factor, f, discussed earlier.

A listing of the computer program used for the final calculations is included in Appendix B.

It should be clear from the above analyses that much work remains to be accomplished before accurate and reliable predictions of side forces and moments can be made. This area of research is presently being pursued by the Navy, Air Force, Army, and NASA and, hopefully, better methods will be available in the near future.

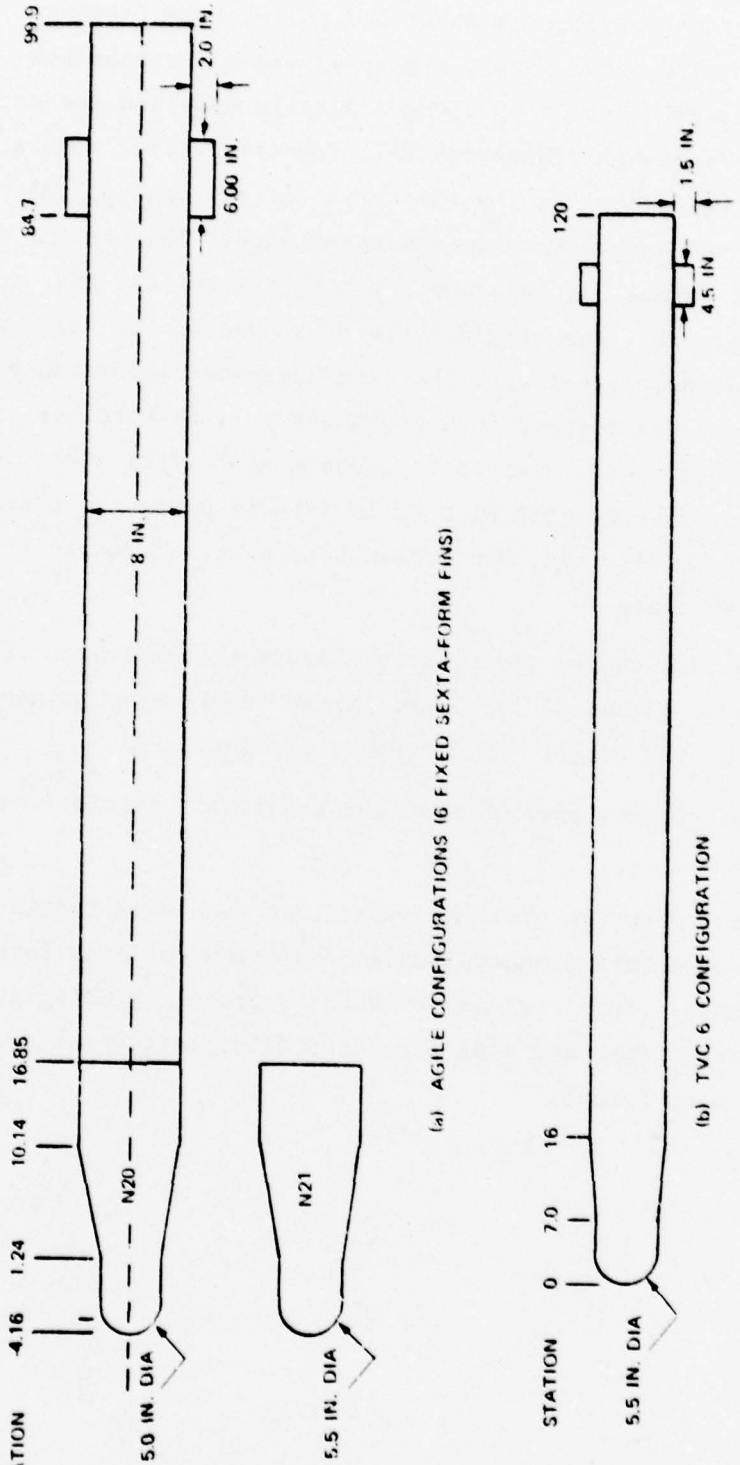

FIGURE 1. Agile and TVC6 Missile Configurations.

20

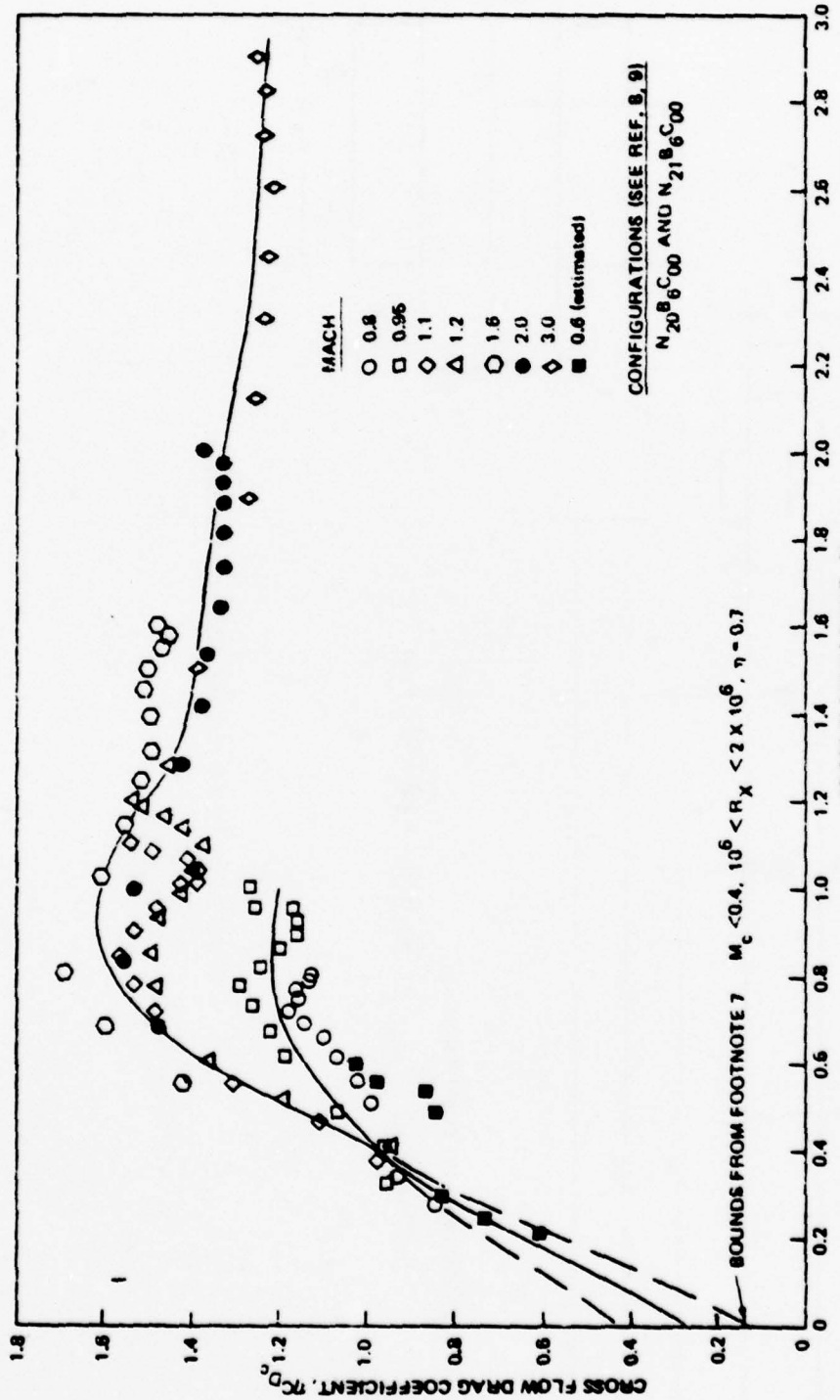

FIGURE 2. Correlation of Cross Flow Drag Coefficient vs Cross Flow Mach Number for Agile.

21

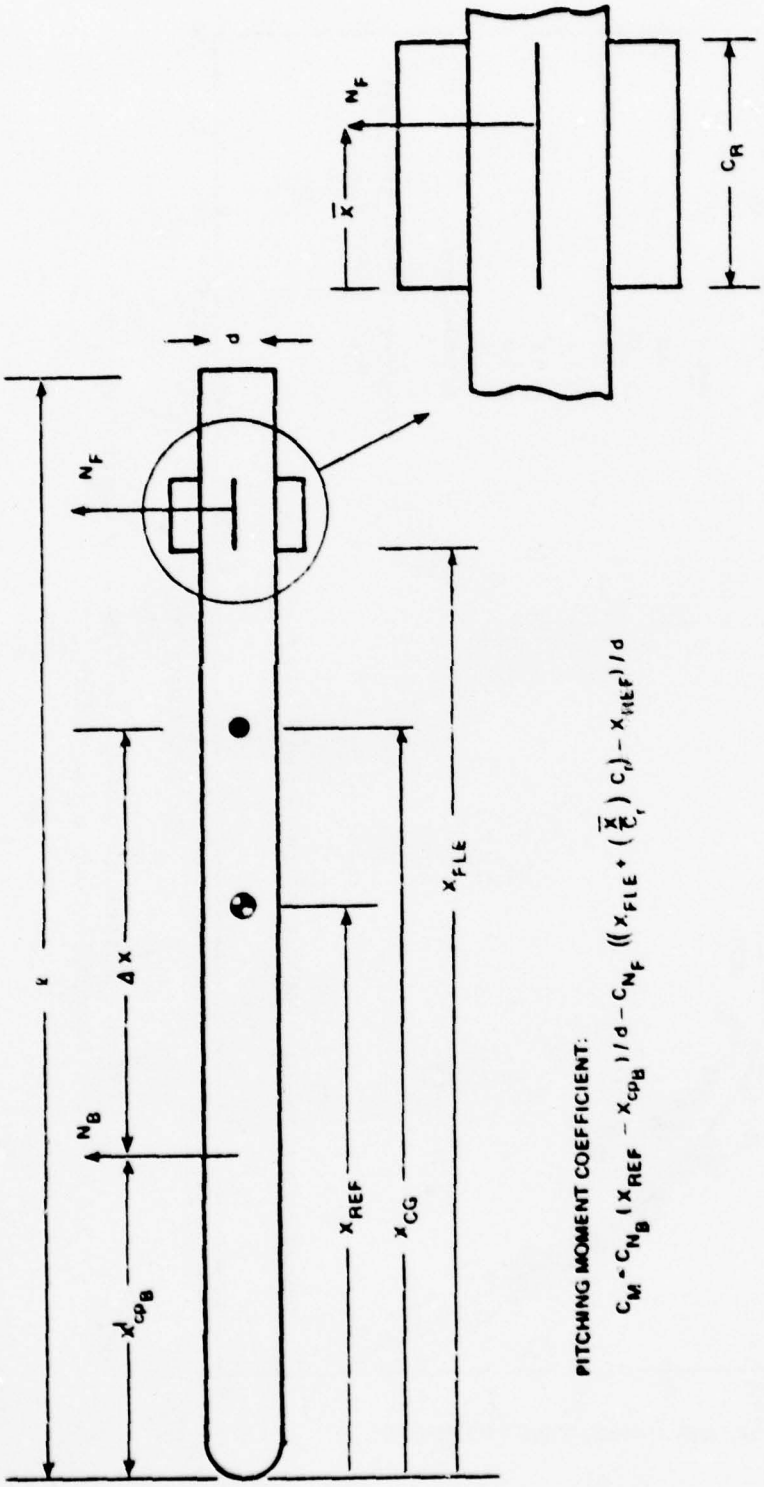

PITCHING MOMENT COEFFICIENT:

$$C_M = C_{N_B}\left[X_{REF} - X_{CP_B}\right]/d - C_{N_F}\left[\left(X_{FLE} + \left(\frac{\bar{X}}{C_r}\right) C_r\right) - X_{REF}\right]/d$$

FIGURE 3. TVC6 Moment Calculations.

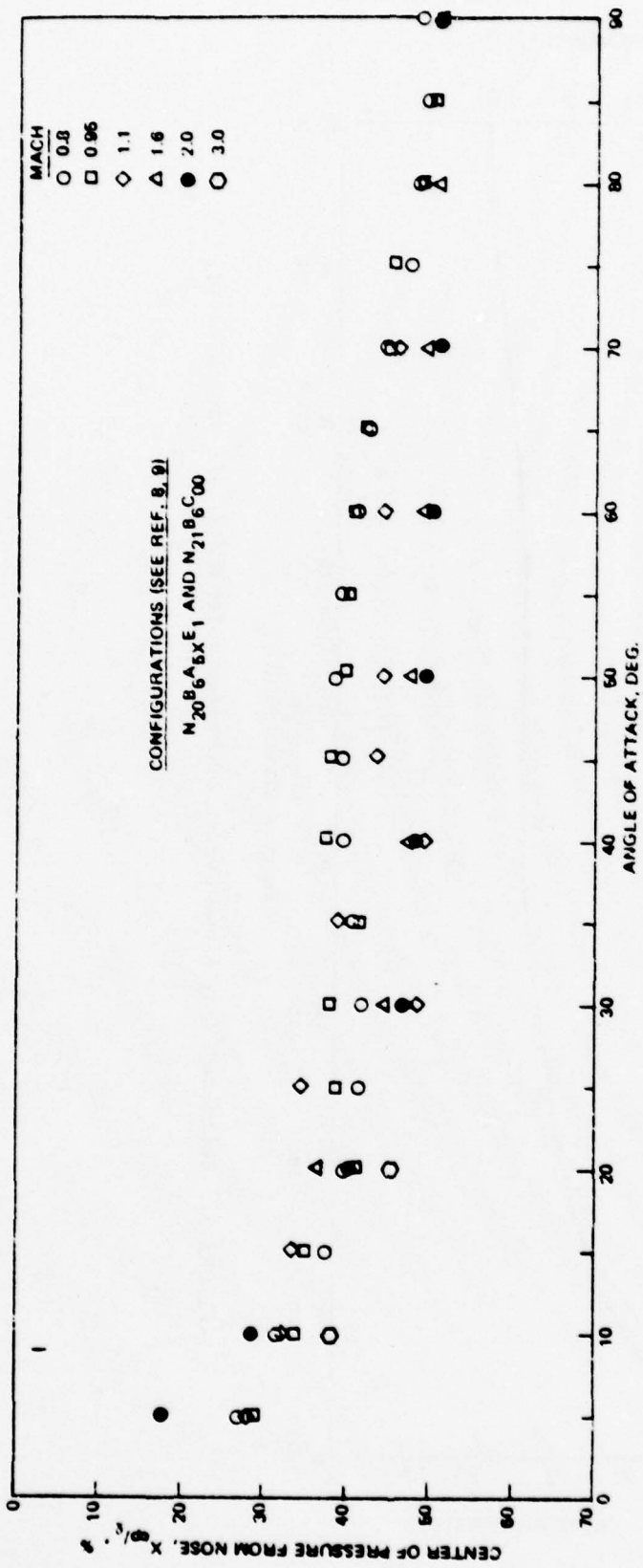

FIGURE 4. Center of Pressure for Agile Configurations.

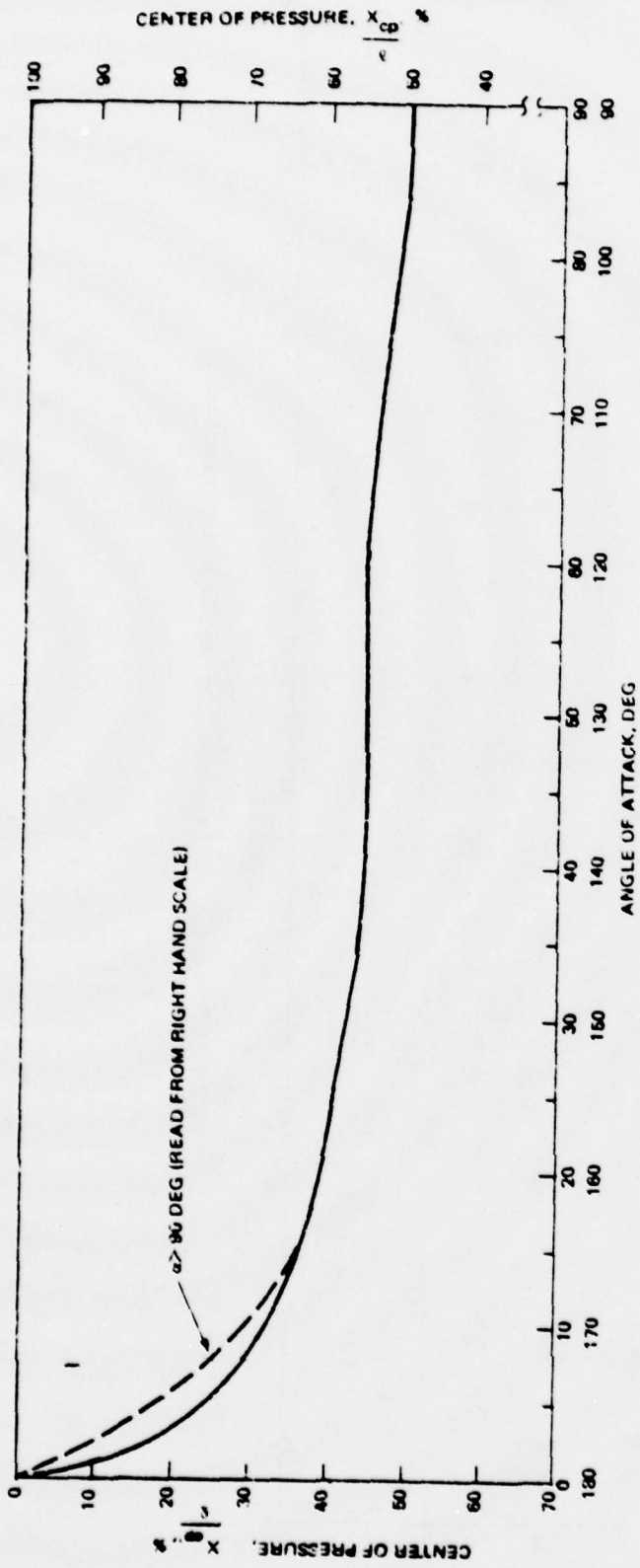

FIGURE 5. Estimated Body Alone Center of Pressure for TVC6, All Mach Numbers.

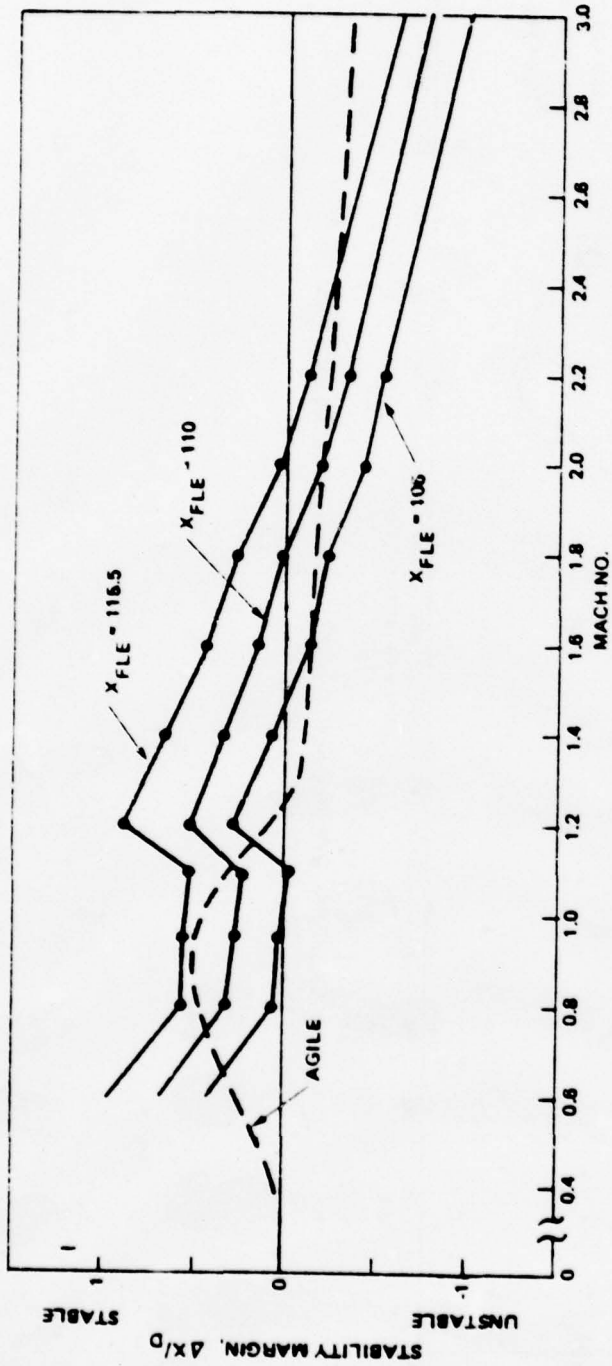

FIGURE 6. Comparison of Agile and TVC6 Launch Static Stability Margins.

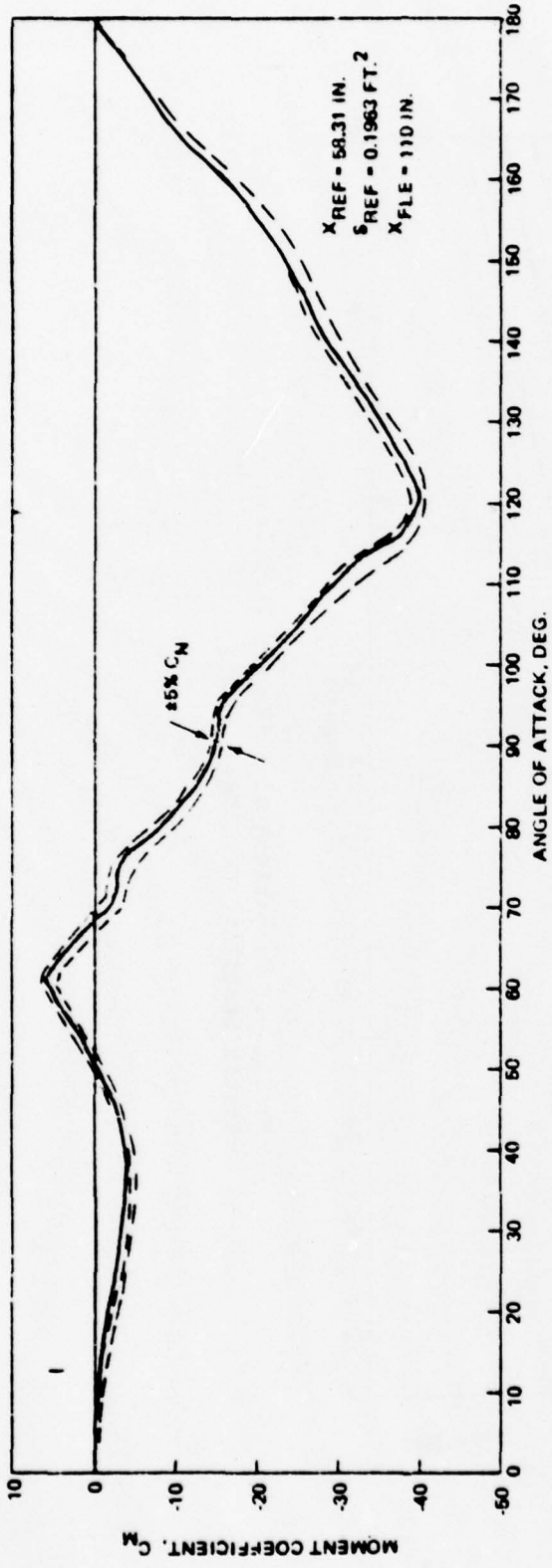

FIGURE 7. TVC6 Moment Coefficient Sensitivity to Body Normal Force Coefficient, C_{N_B} (Mach = 0.8).

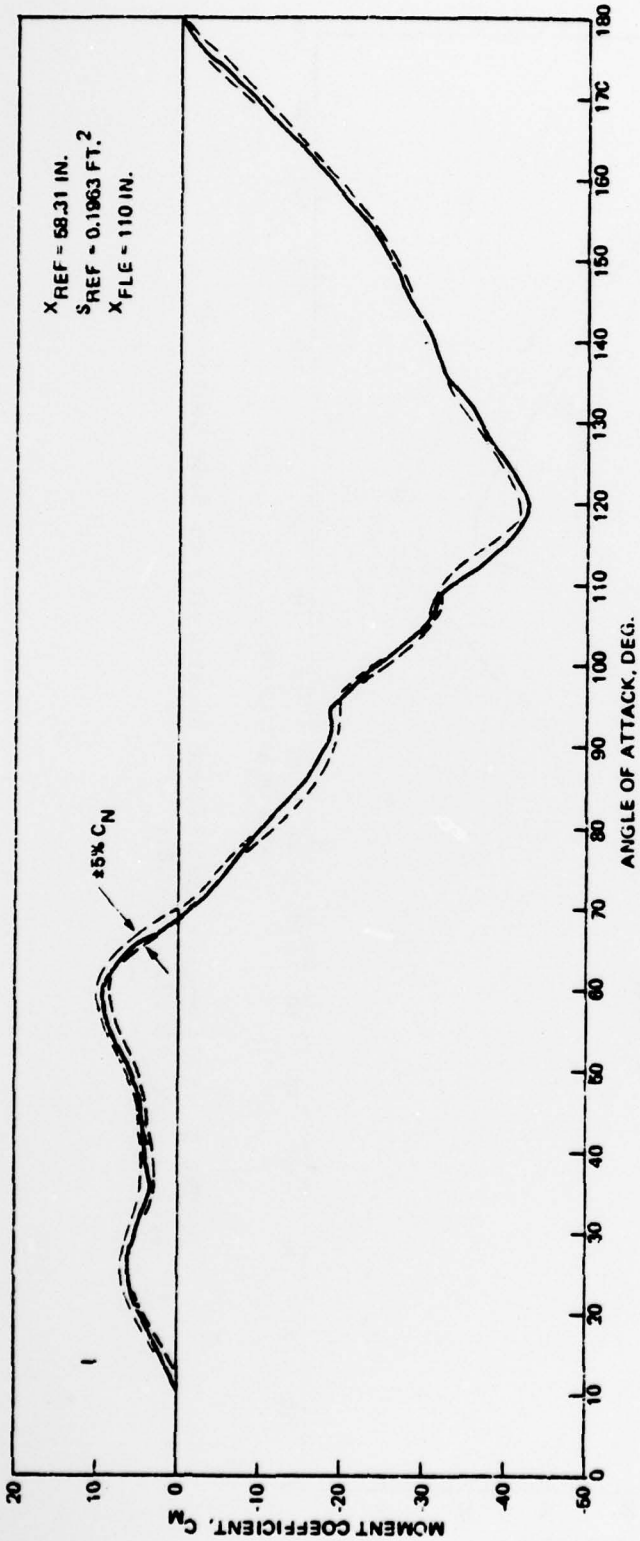

FIGURE 8. TVC6 Moment Coefficient Sensitivity to Body Normal Force Coefficient, C_{N_B} (Mach = 2.0).

27

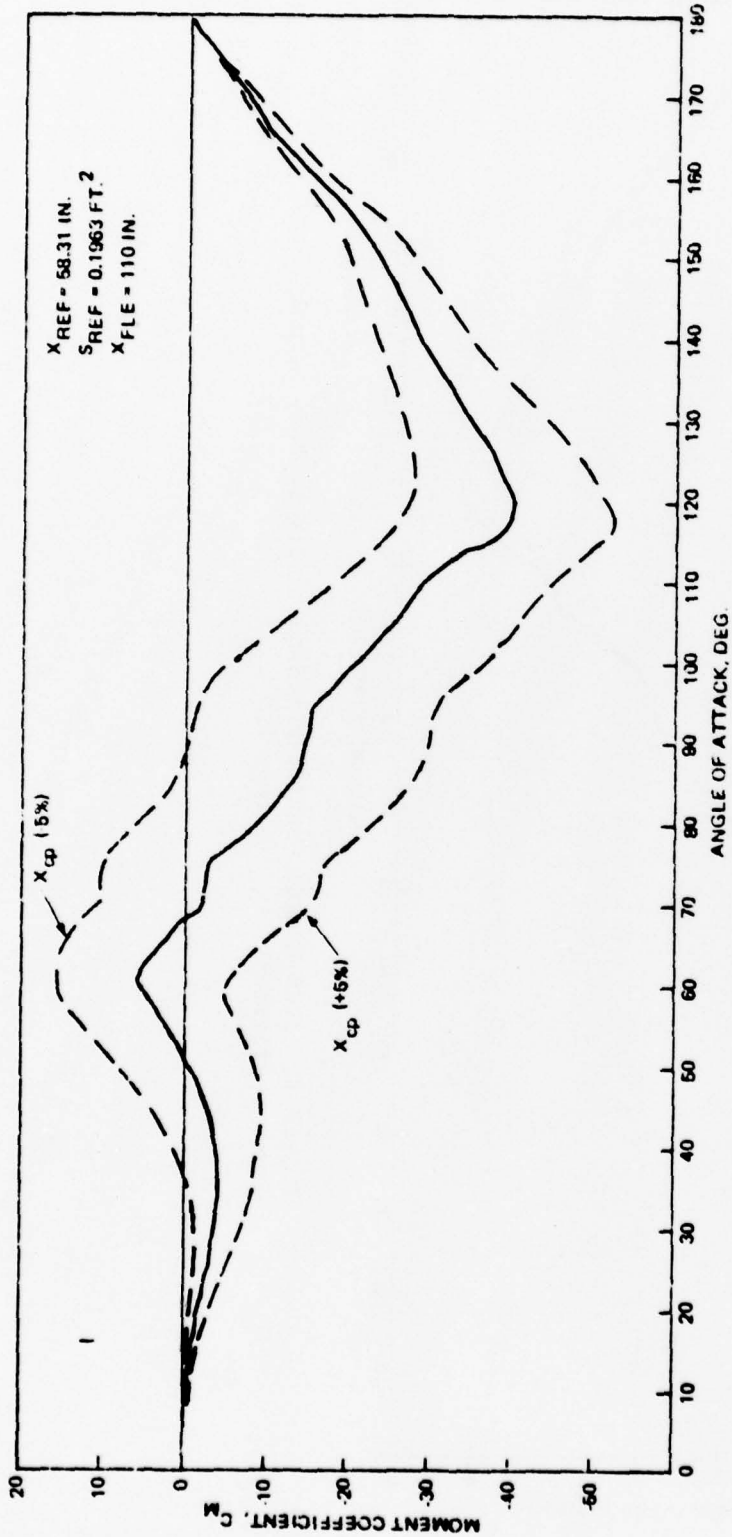

FIGURE 9. TVC6 Moment Coefficient Sensitivity to Body Center of Pressure, X_{cp}/ℓ (Mach = 0.8).

28

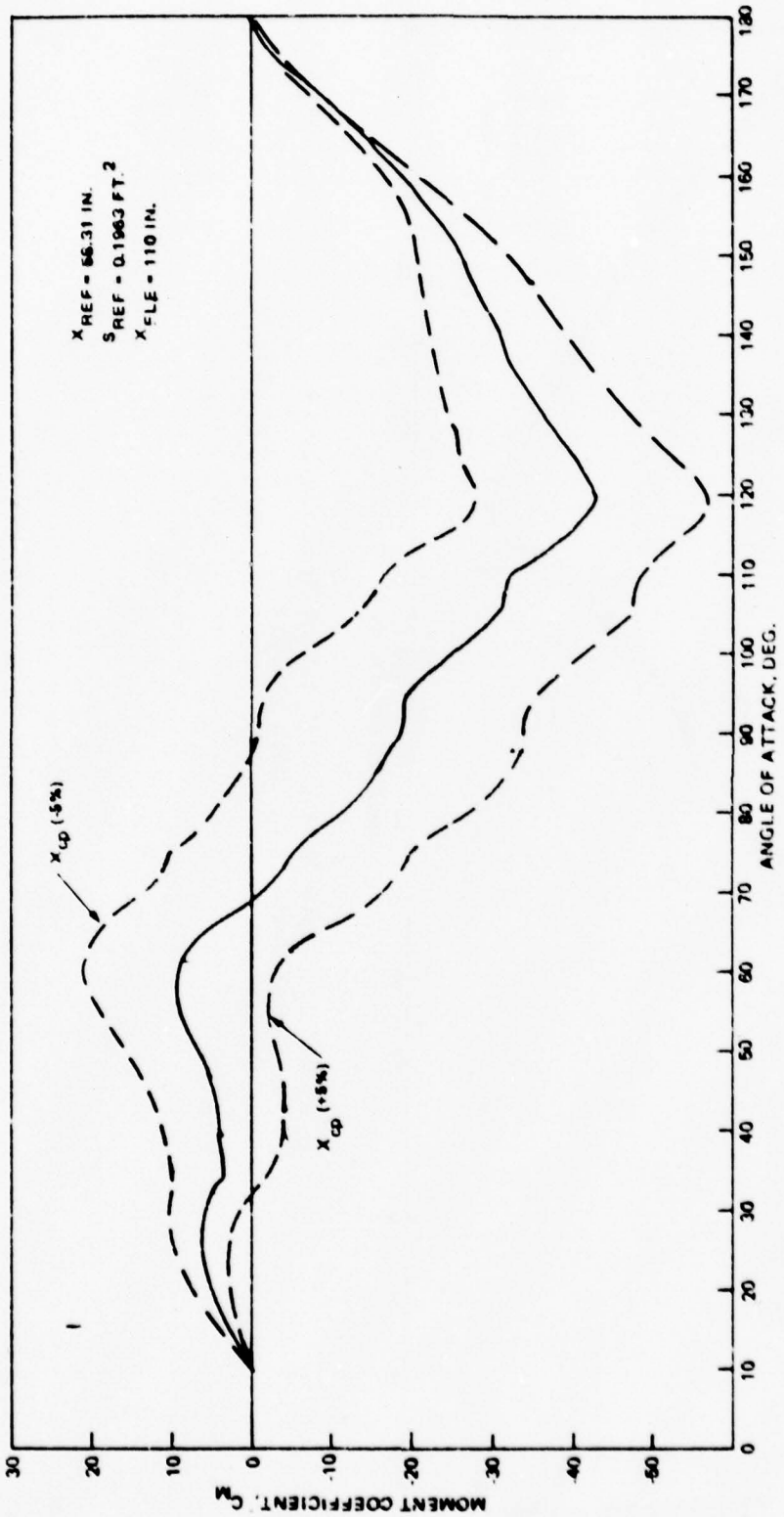

FIGURE 10. TVC6 Moment Coefficient Sensitivity to Body Center of Pressure, X_{cp}/ℓ (Mach = 2.0).

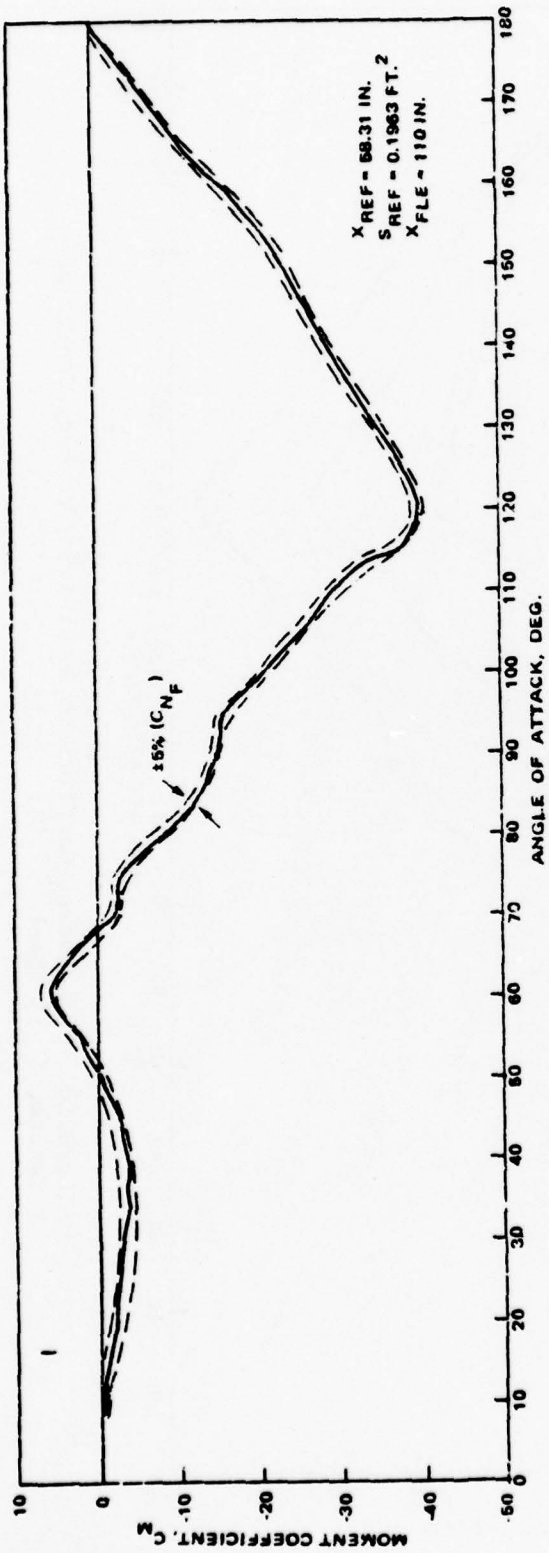

FIGURE 11. TVC6 Moment Coefficient Sensitivity to Fin Normal Force, C_{N_F} (Mach = 0.8).

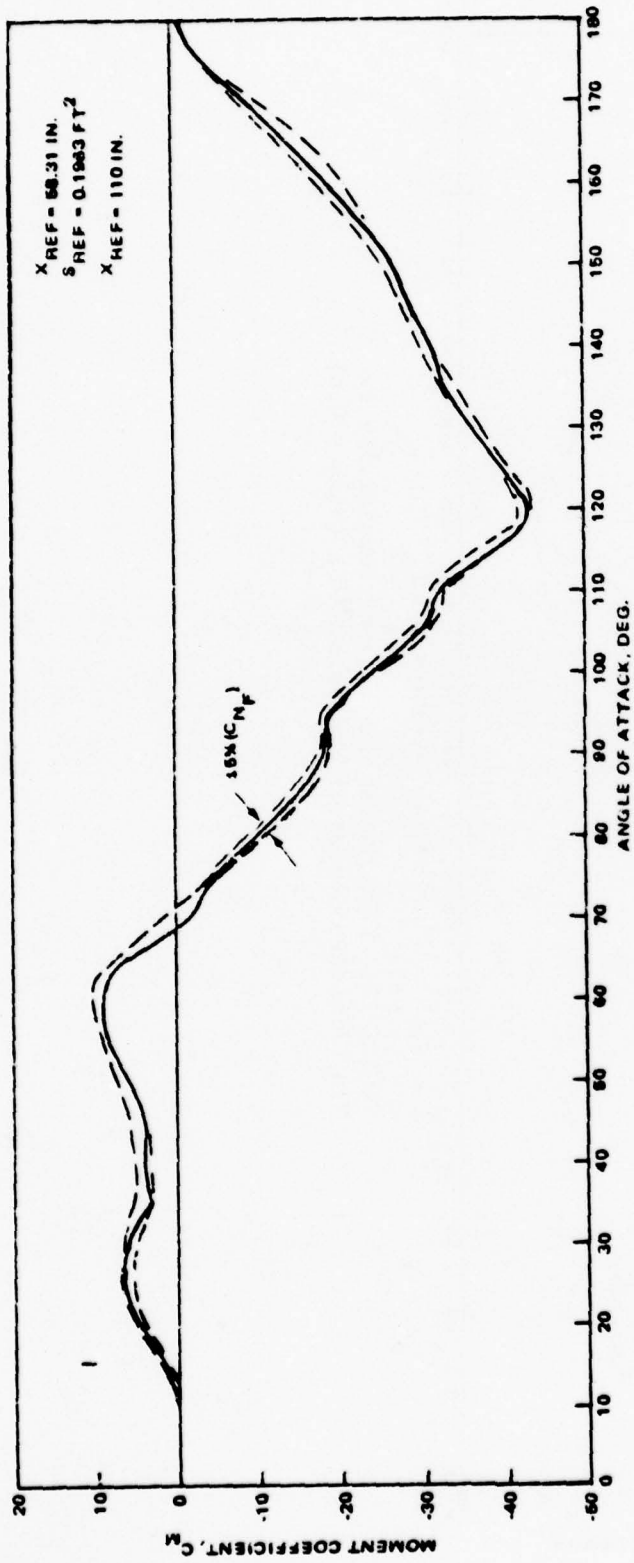

FIGURE 12. TVC6 Moment Coefficient Sensitivity to Fin Normal Force, C_{N_F} (Mach 2.0).

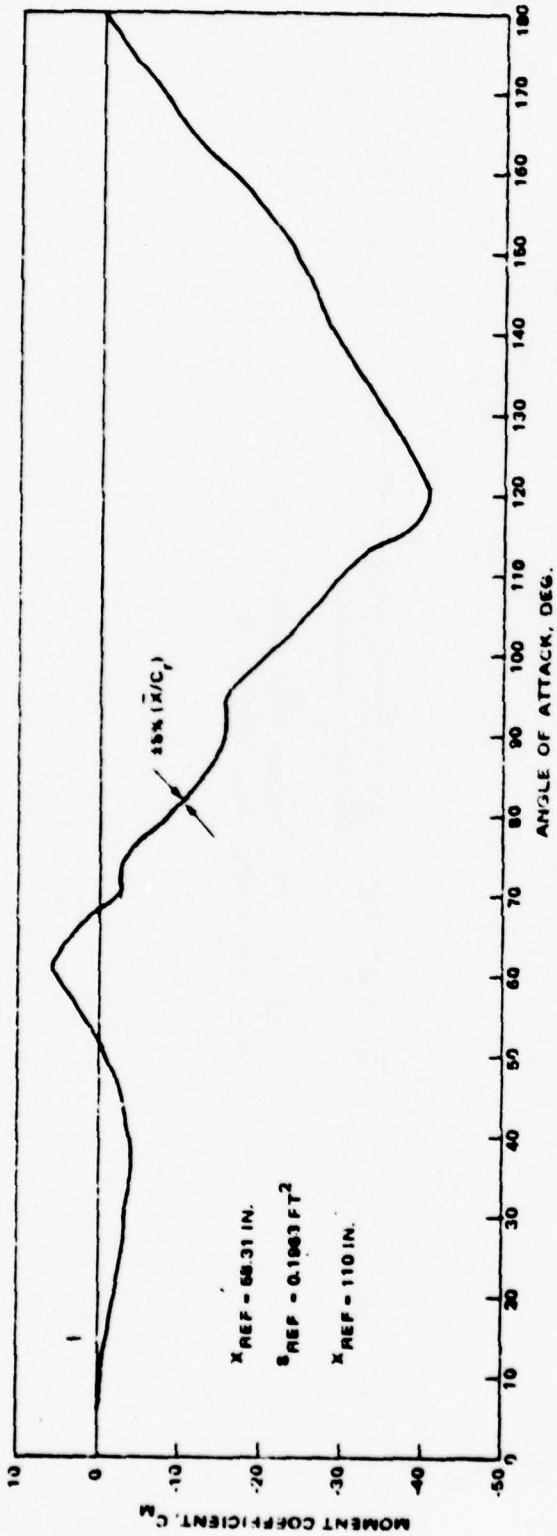

FIGURE 13. TVC6 Moment Coefficient Sensitivity to Fin Effective Center of Pressure, $\bar{X}/C_r$ (Mach = 0.8).

32

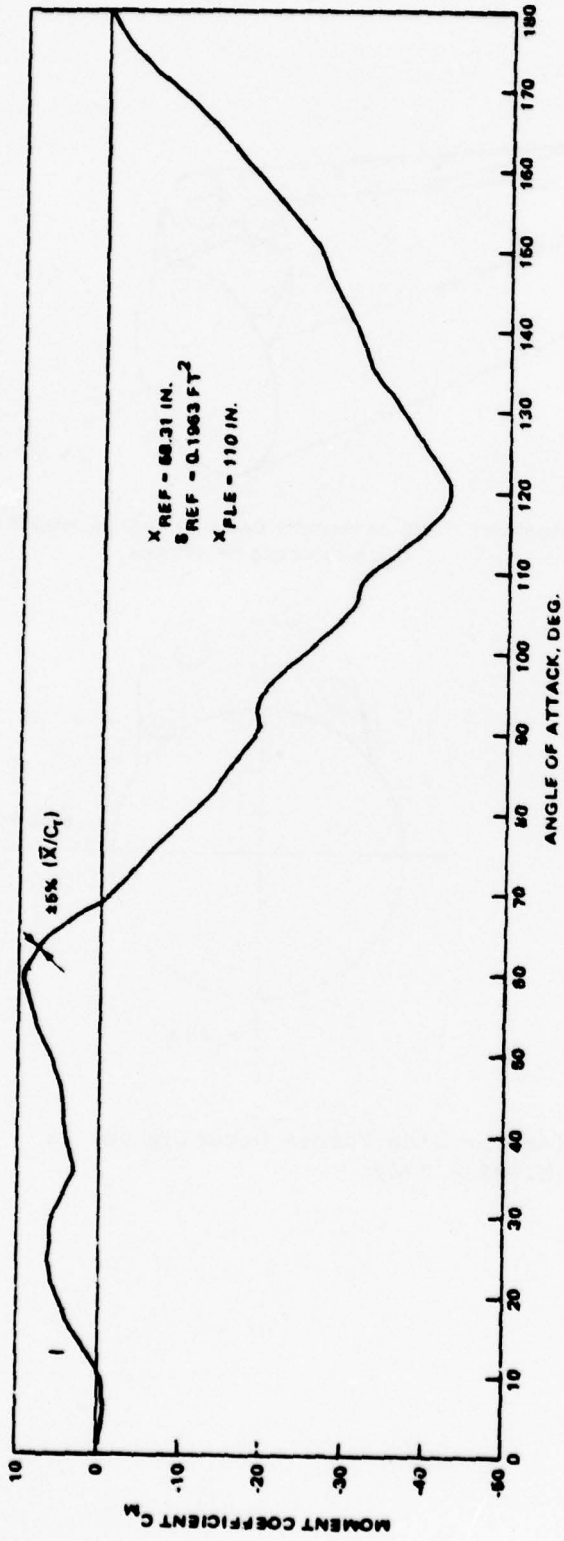

FIGURE 14. TVC6 Moment Coefficient Sensitivity to Fin Effective Center of Pressure, $\bar{X}/C_r$ (Mach = 2.0).

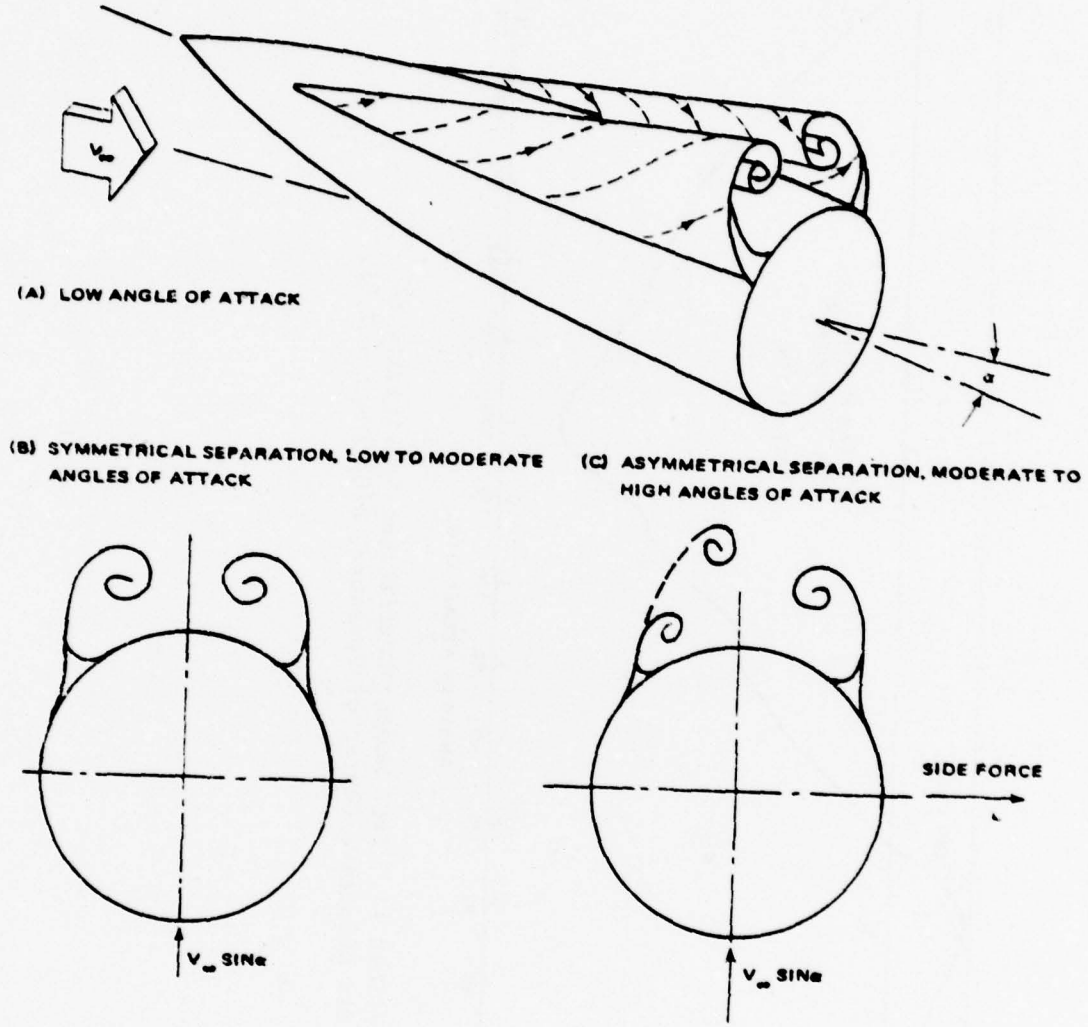

FIGURE 15. Out-of-Plane or Side Forces Occuring Due to Flow Separation on a Missile Body.

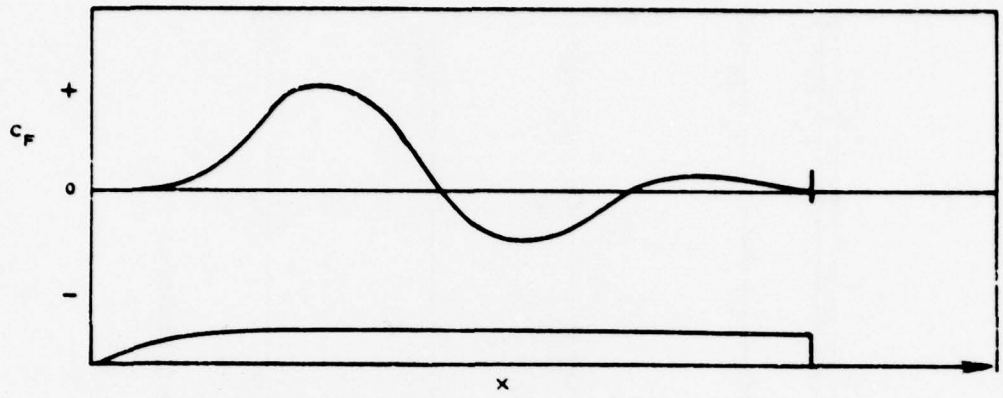

FIGURE 16. Typical Side Force Distribution at a Fixed Angle of Attack.

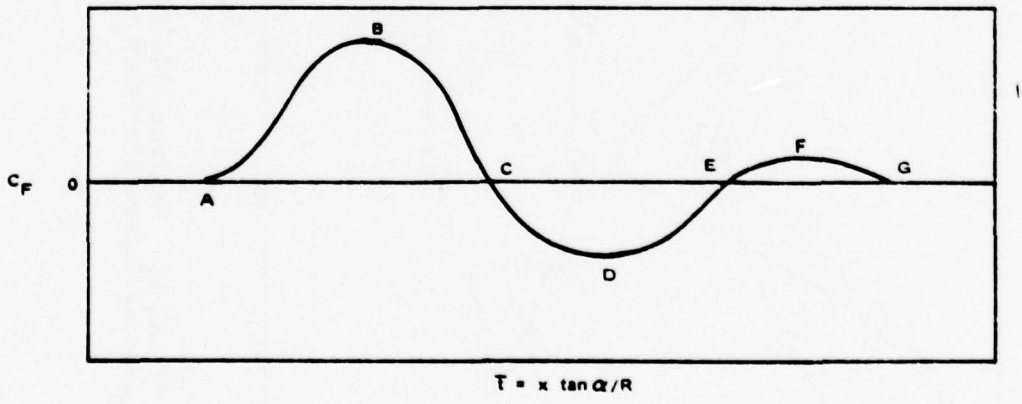

FIGURE 17. Characteristic Distribution of Side Force Along the Body (From Reference 6).

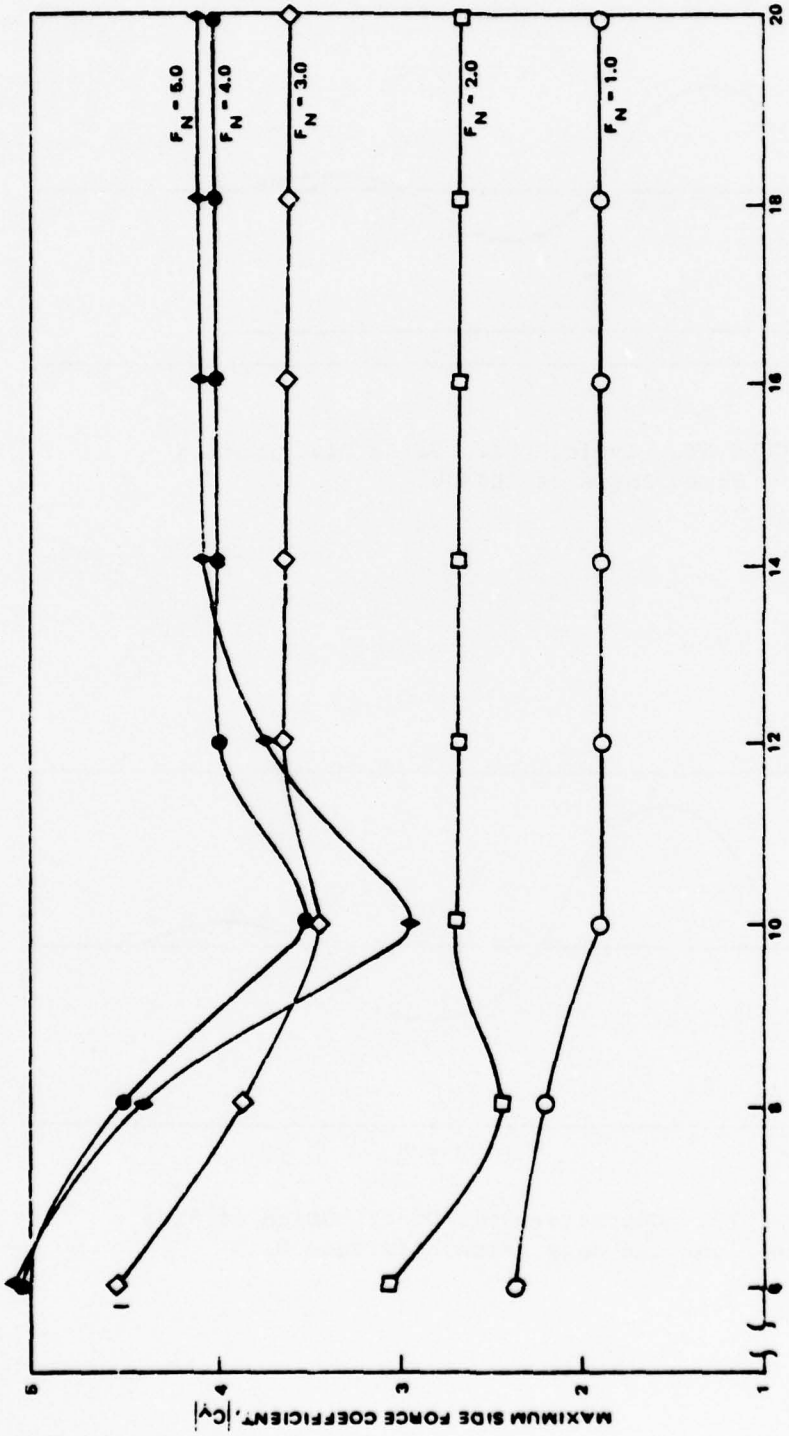

FIGURE 18. Maximum Side Force Coefficient for Ogive Cylinders, Laminar Separation (Mach = 0)(From Reference 6).

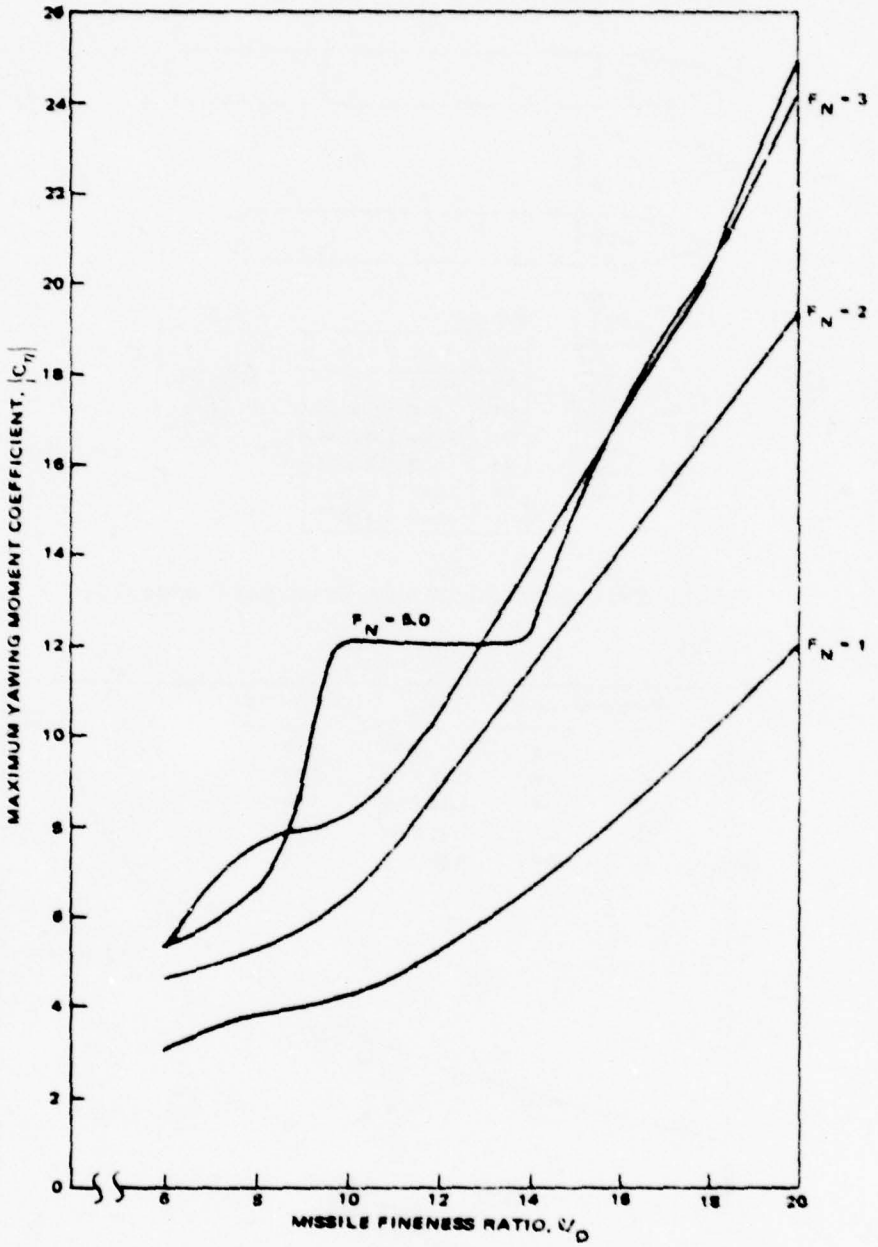

FIGURE 19. Maximum Yawing Moment Coefficient for Ogive Cylinders, Laminar Separation (Mach = 0; Moment Center at Mid-Body) (From Reference 6).

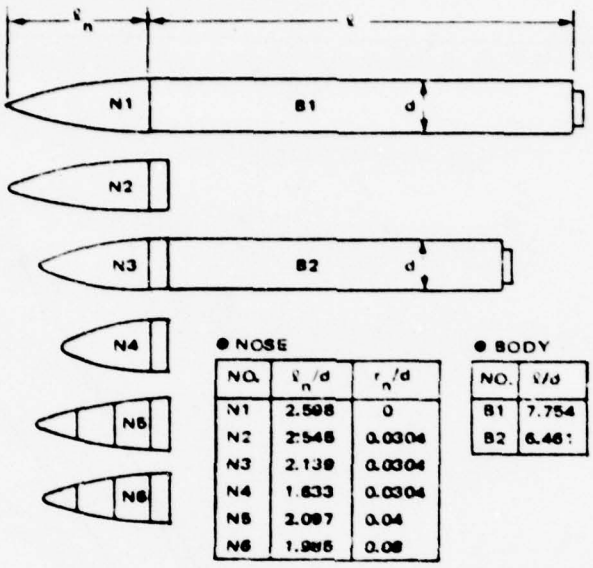

● NOSE

NO.	ℓ_n/d	r_n/d
N1	2.598	0
N2	2.546	0.0304
N3	2.139	0.0304
N4	1.633	0.0304
N5	2.097	0.04
N6	1.995	0.08

● BODY

NO.	ℓ/d
B1	7.754
B2	6.461

FIGURE 20. Configurations From Reference 10.

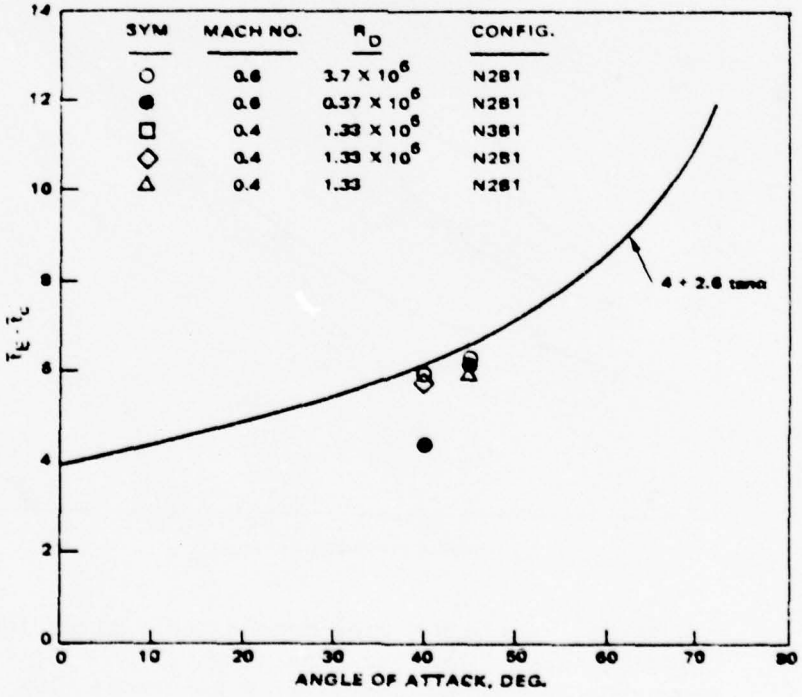

FIGURE 21. Comparison of Theoretical Spacing Parameters With Data From Reference 10.

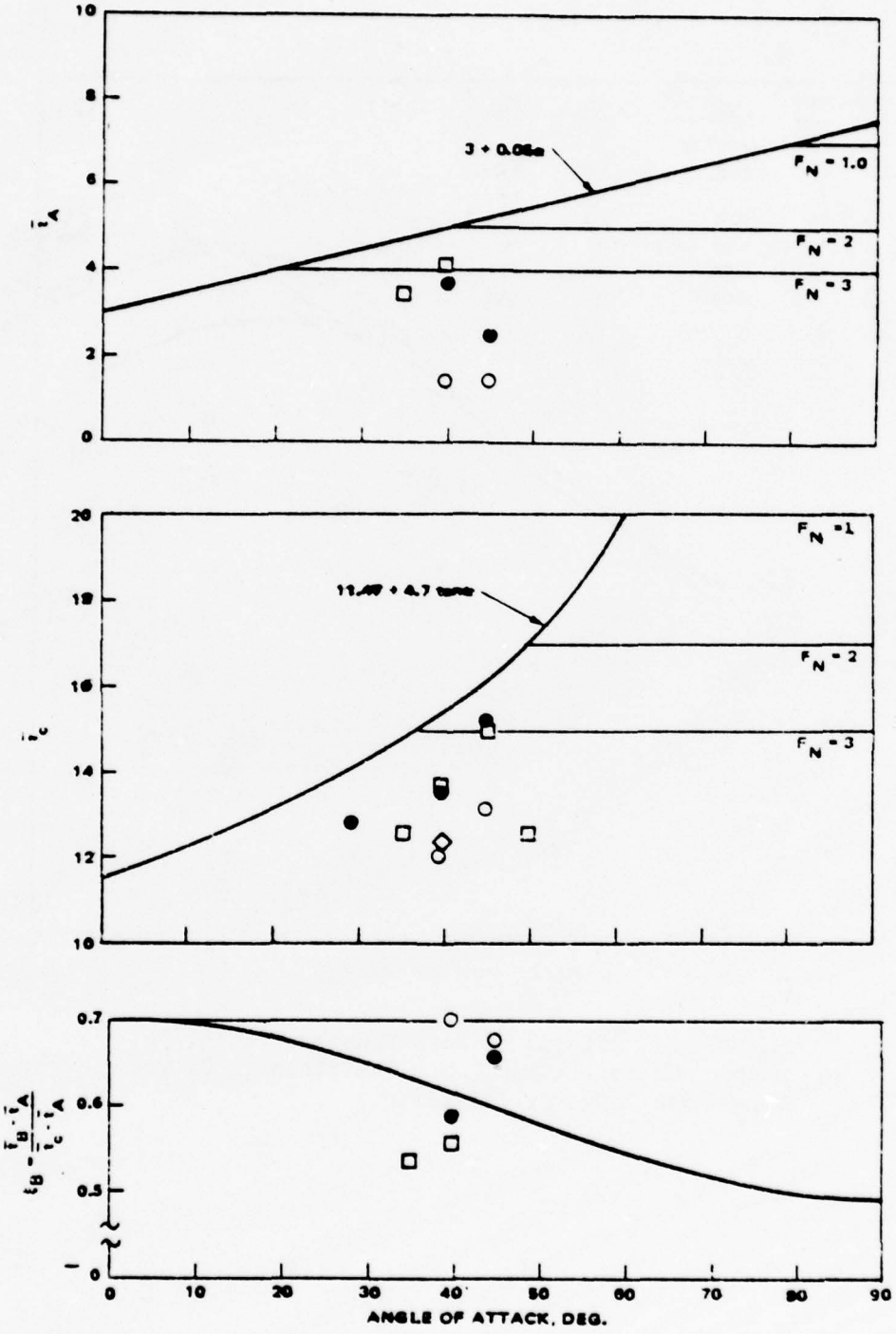

FIGURE 21. (Contd.)

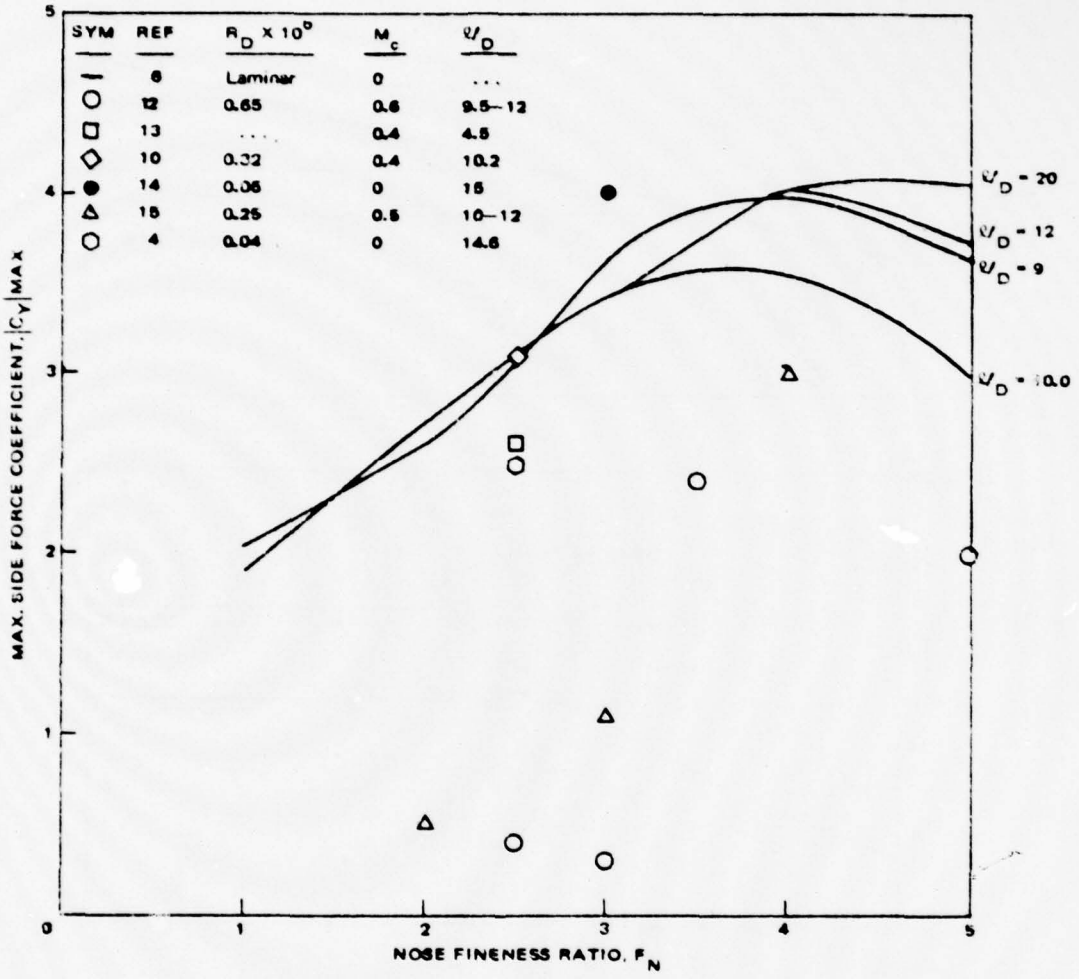

FIGURE 22. Effects of Nose Fineness Ratio, F_N, on Maximum Total Side Force Coefficient, C_Y For Sharp-Nose Ogive Cylinders.

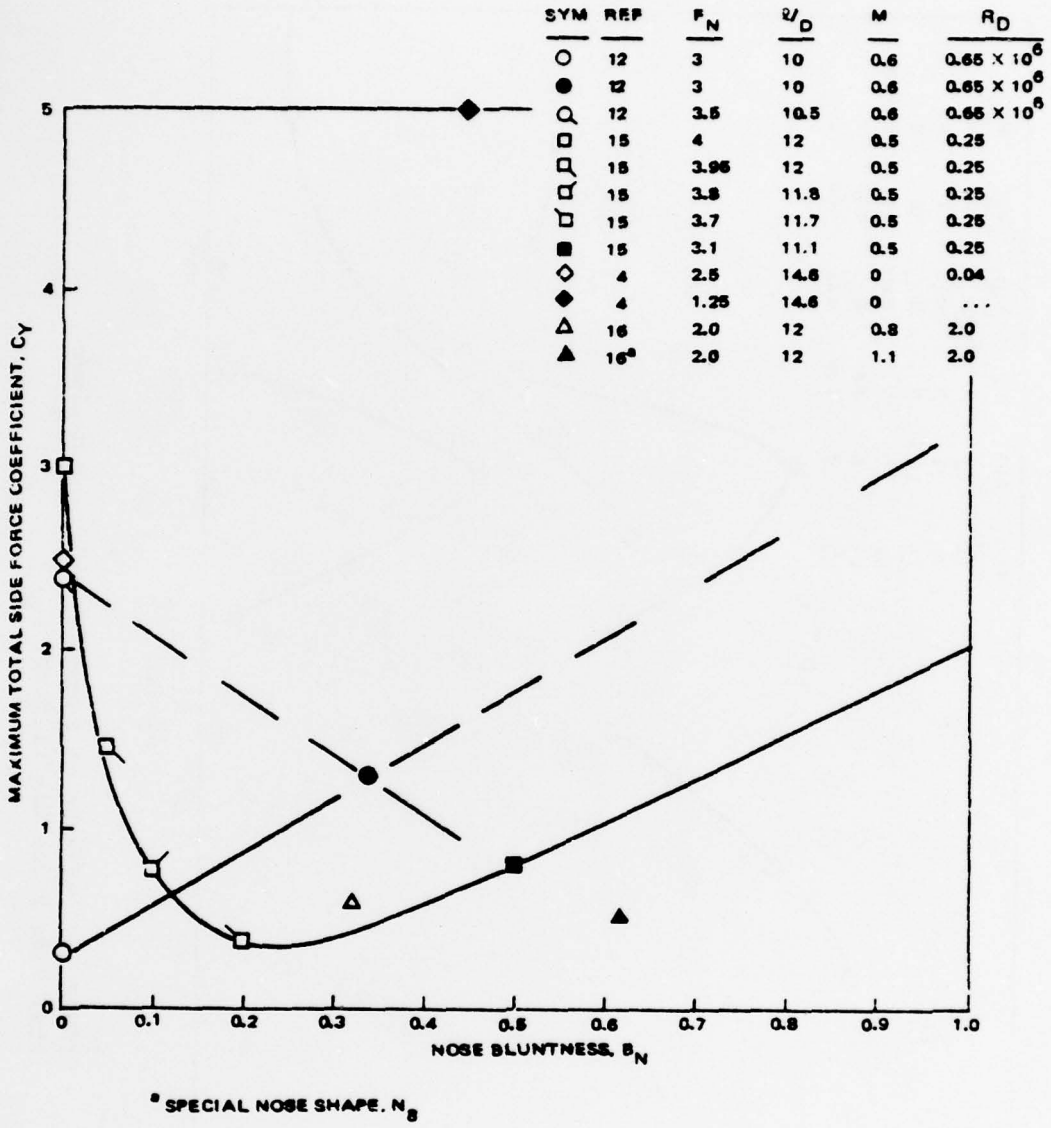

FIGURE 23. Effects of Nose Bluntness, B_N, on Maximum Total Side Force Coefficient, C_Y, For Ogive Cylinders.

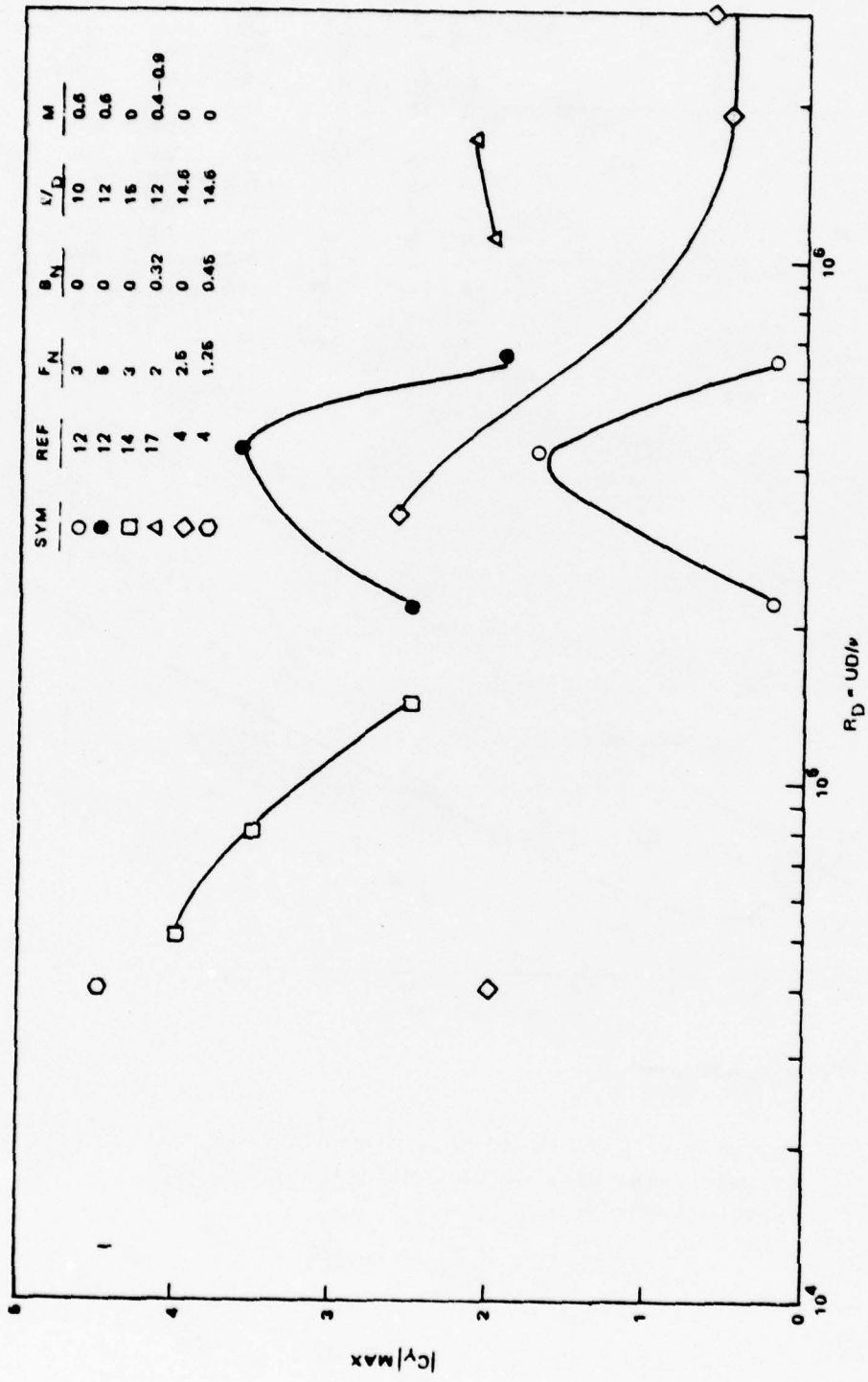

FIGURE 24. Effects of Reynolds Number on Maximum Total Side Force Coefficient, C_Y.

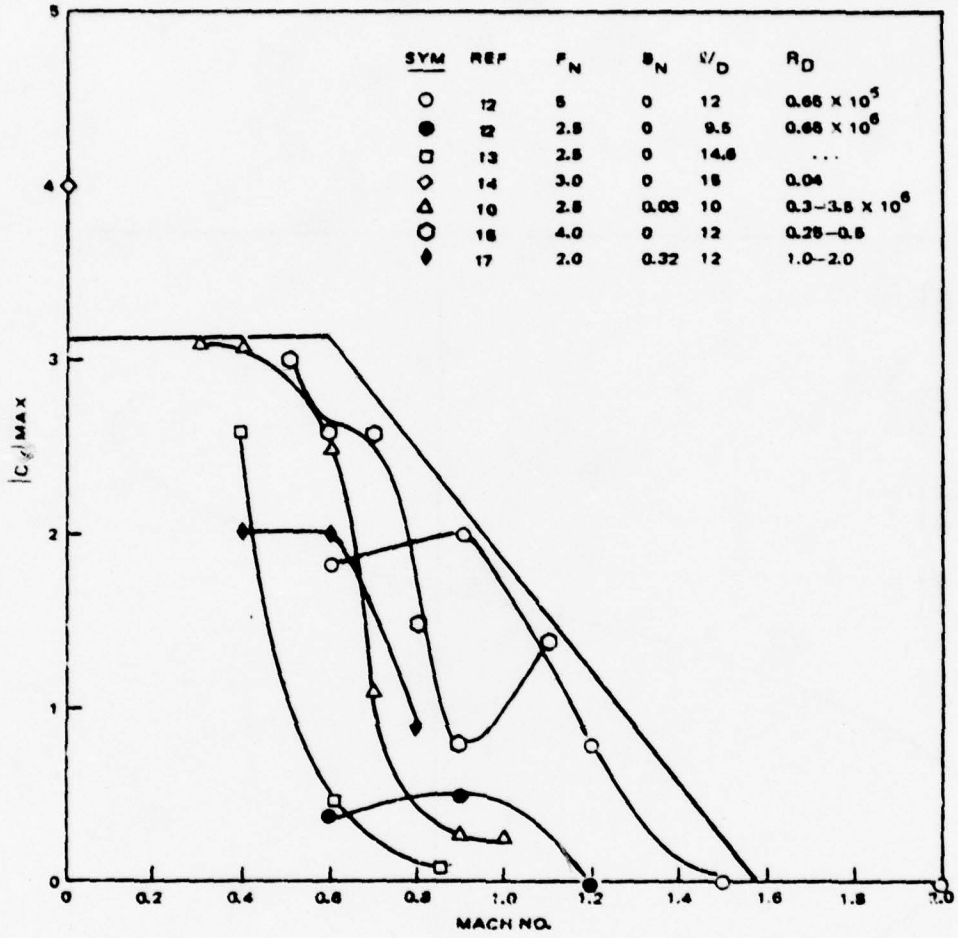

FIGURE 25. Effects of Mach Number on Maximum Total Side Force Coefficient, C_Y.

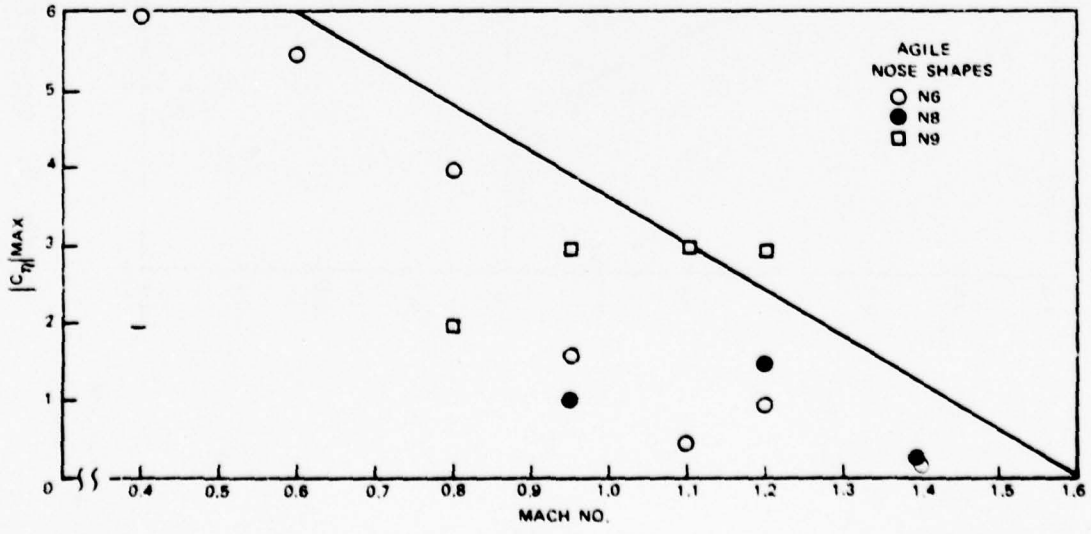

FIGURE 26. Effect of Mach Number and Nose Shape on Maximum Yawing Moment Coefficient, Agile (See References 16 and 17).

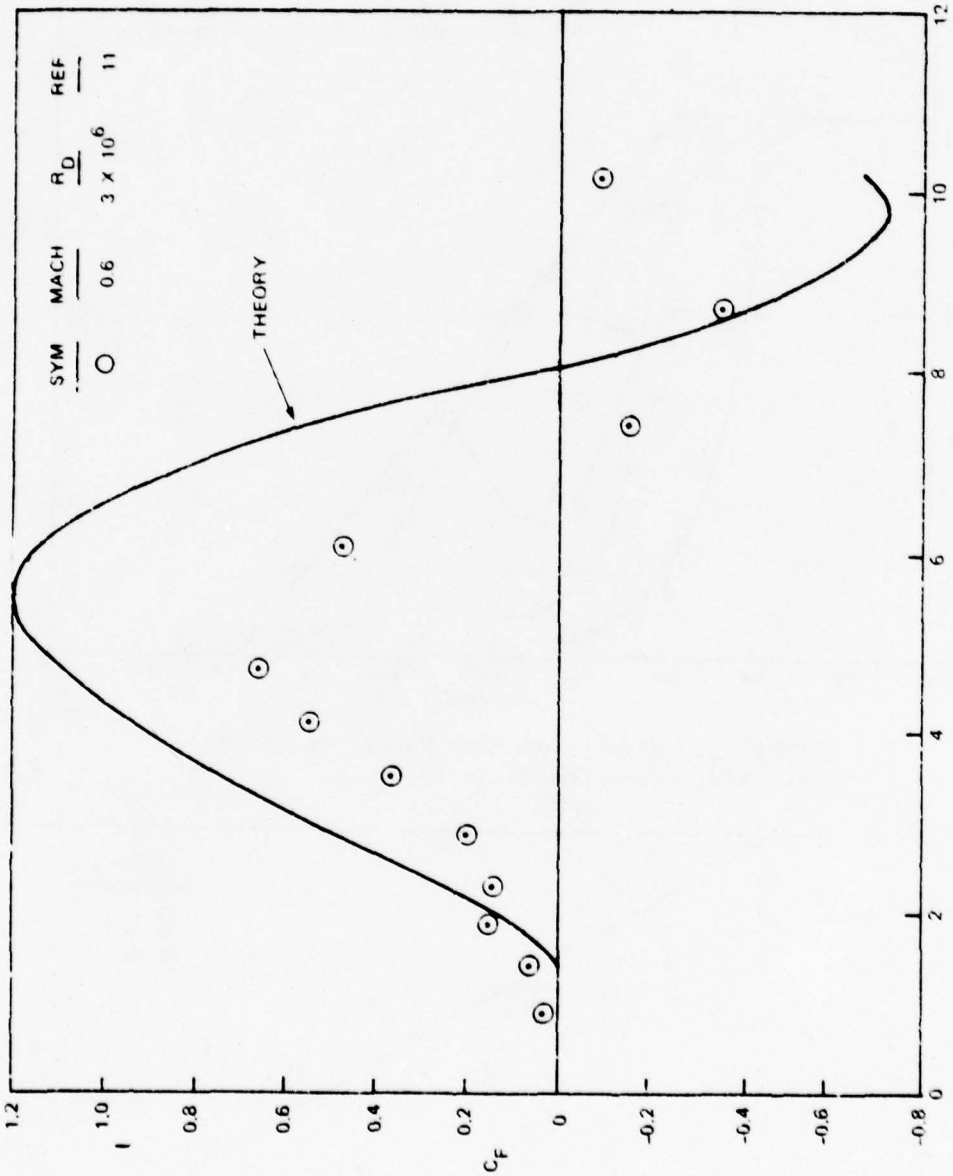

FIGURE 27. Out-of-Plane Force Distribution at 40-Degree Angle of Attack.

44

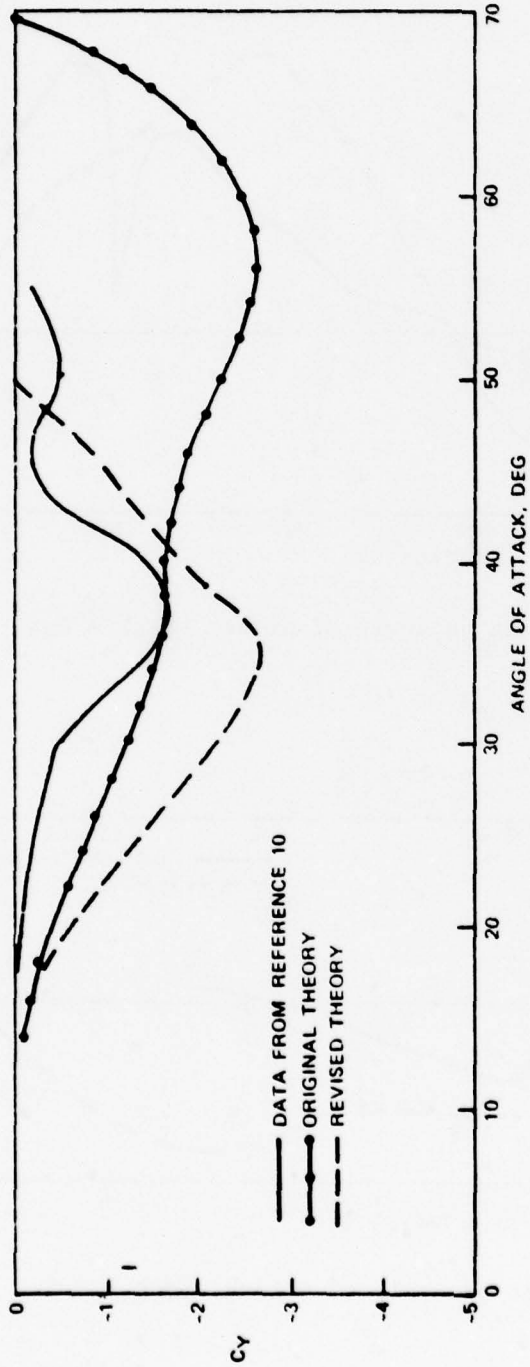

FIGURE 28. Side Force Coefficient vs Angle of Attack, Data From Reference 10.

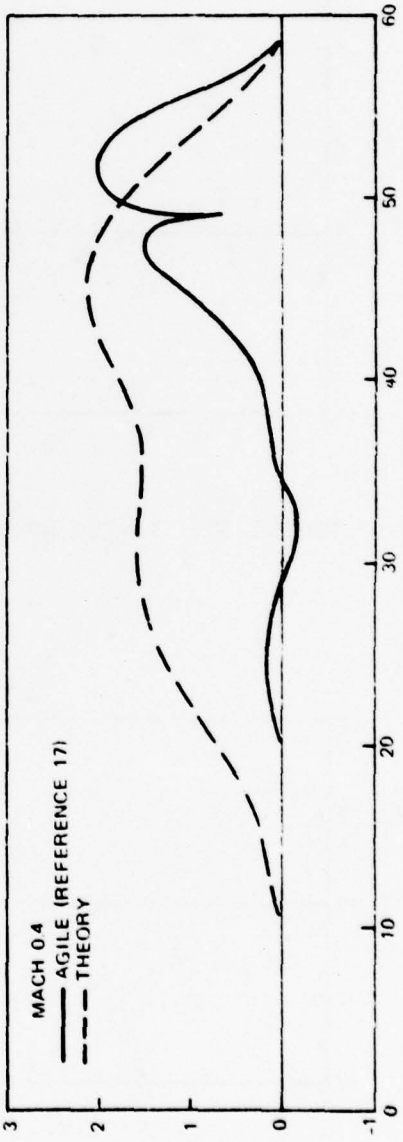

FIGURE 29. Side Force Coefficient vs Angle of Attack, Mach = 0.4.

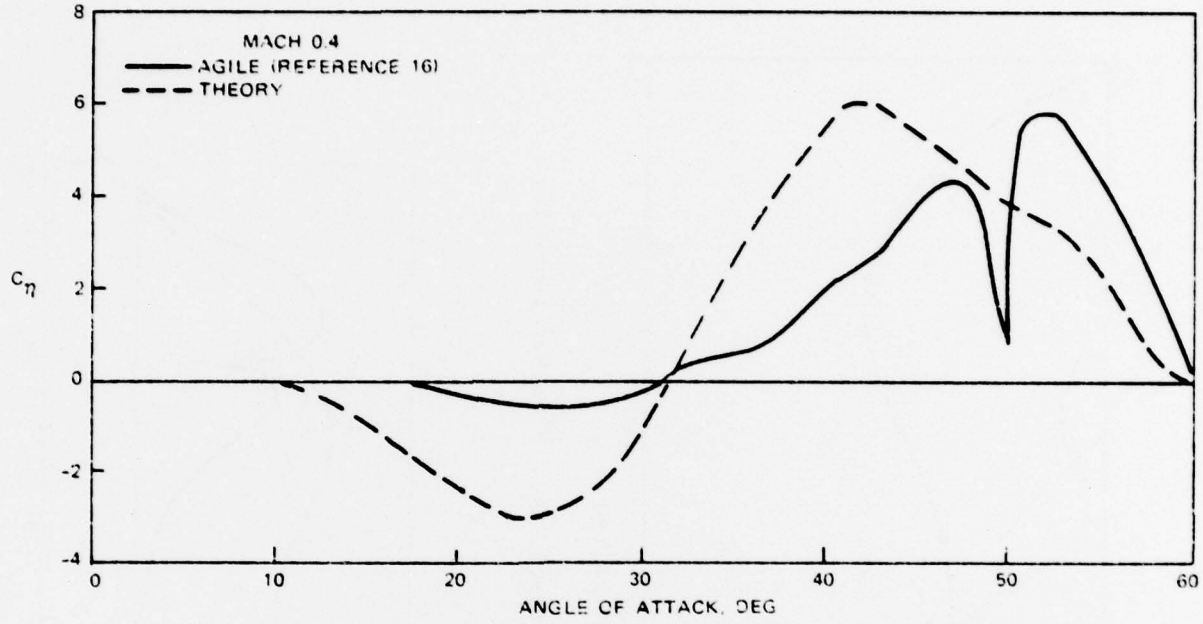

FIGURE 30. Yawing Moment Coefficient vs Angle of Attack, Mach = 0.4.

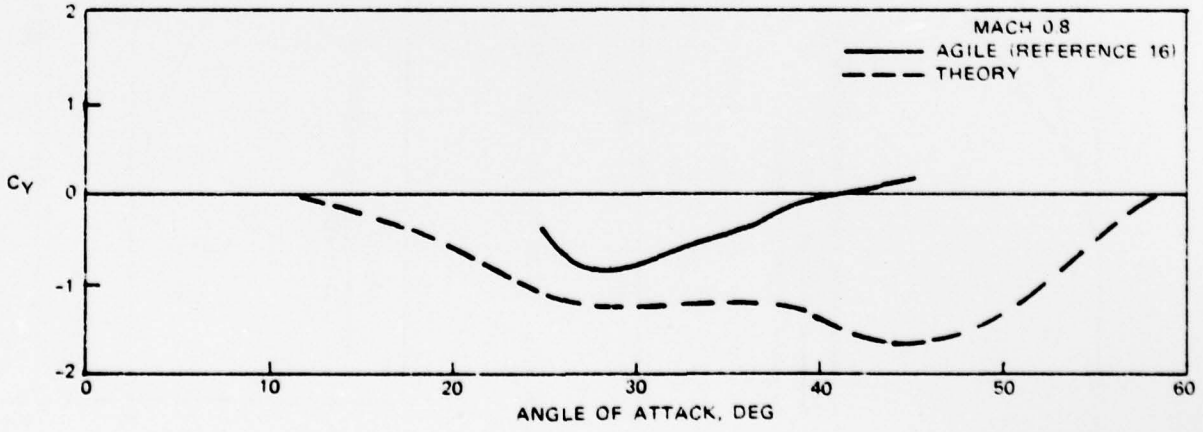

FIGURE 31. Side Force Coefficient vs Angle of Attack, Mach = 0.8.

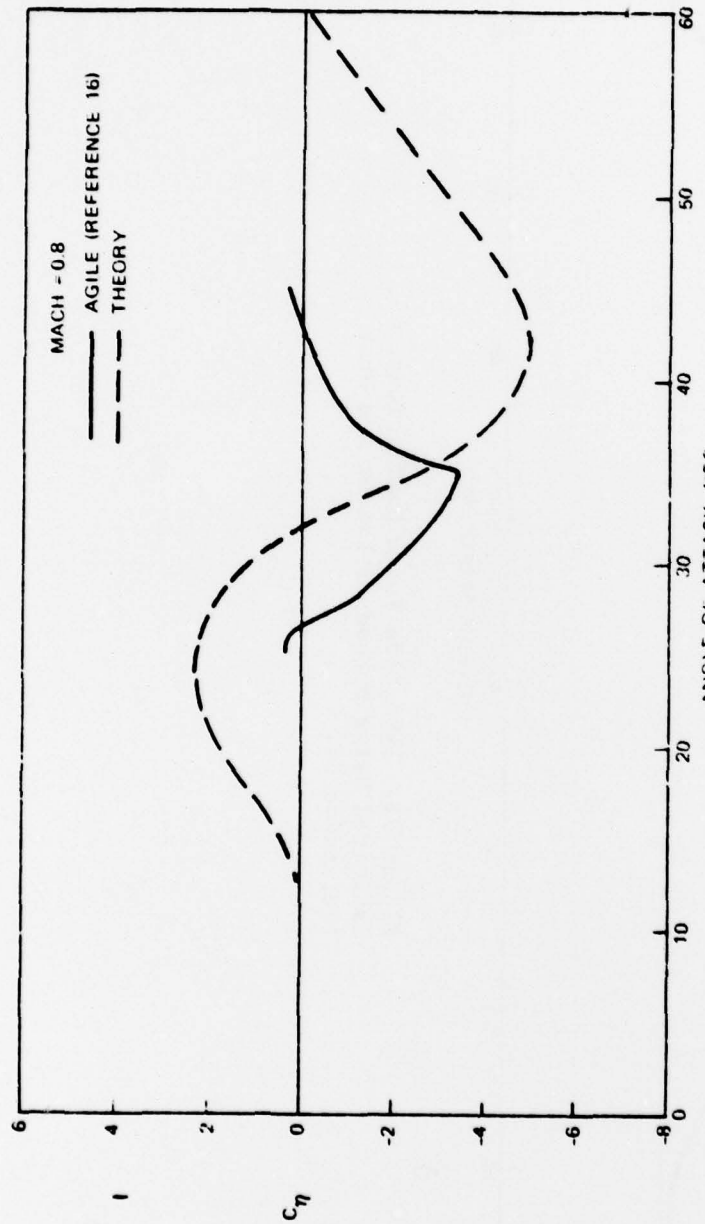

FIGURE 32. Yawing Moment Coefficient vs Angle of Attack, Mach = 0.8.

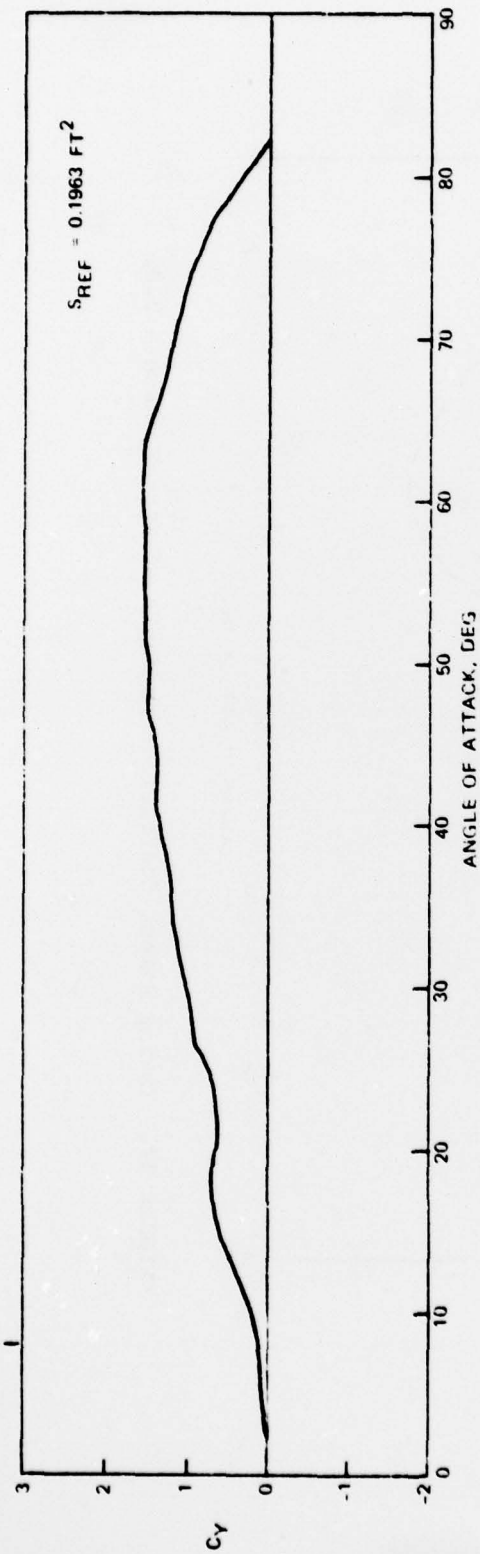

FIGURE 33. TVC6 Side Force Coefficient, C_Y, Estimated Using Method of Lamont and Hunt (Reference 6).

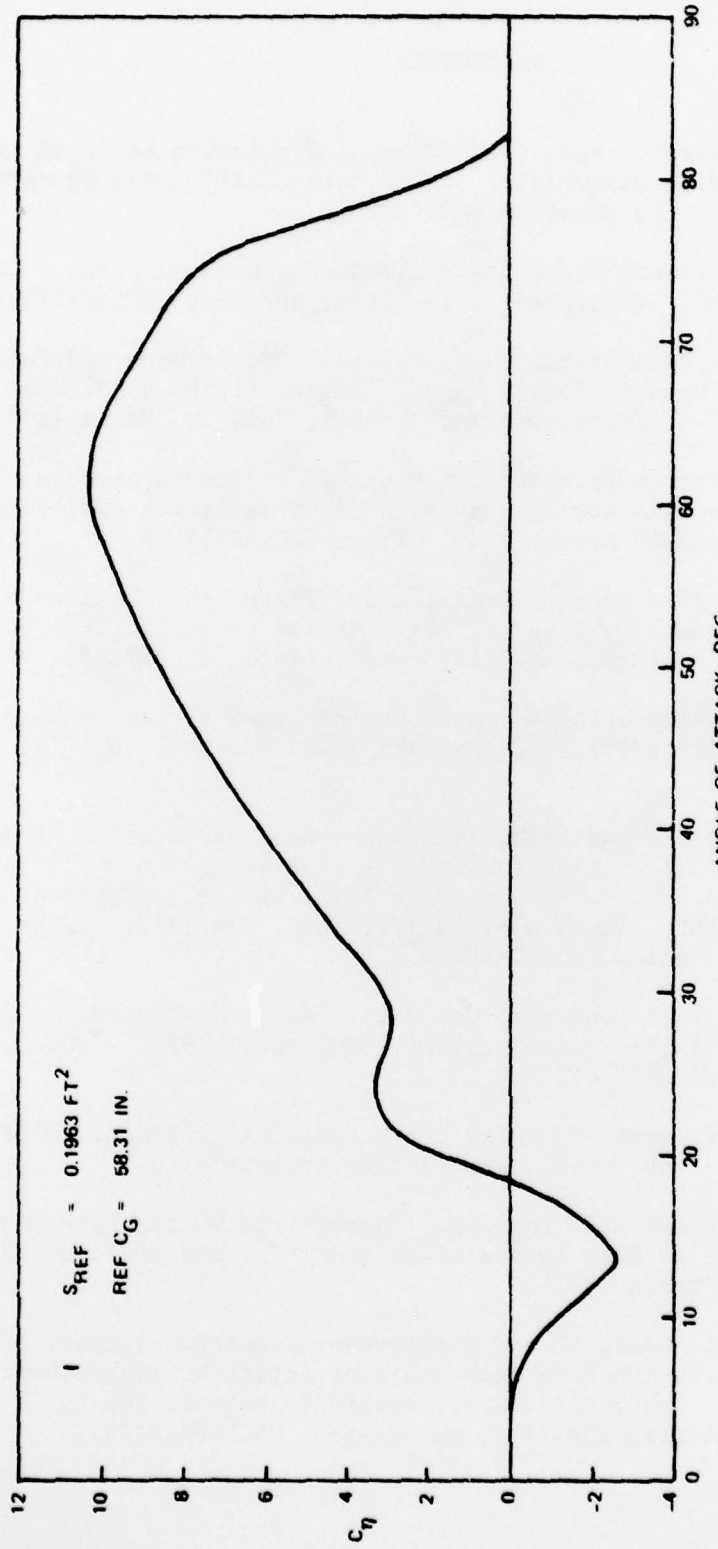

FIGURE 34. TVC6 Yawing Moment Coefficient, C_η, Estimated Using Method of Lamont and Hunt (Reference 6).

REFERENCES

1. Naval Weapons Center. Need for Review of Simulation Employed at ACM(I) (U), by W.F. Cartwright. China Lake, Calif., NWC 20 April 1977. (Reg. Memo 015/14, document UNCLASSIFIED.)

2. ———. 6" TVC Normal Force Coefficient (U), by W.H. Clark. China Lake, Calif., NWC. (Reg. Memo 3914-93-77, document UNCLASSIFIED.)

3. W.H. Clark, J.R. Peoples, and M.M. Briggs. "Occurrence and Inhibition of Large Yawing Moments During High-Incidence Flight of Slender Missile Configurations," *J. Spacecraft and Rockets*, Vol. 10, No. 8 (1973).

4. ———. "Body Vortex Formation on Missiles in Incompressible Flow," presented at the AIAA 4th Atmospheric Flight Mechanics Conference, Hollywood, Fla., 8-10 August 1977. Paper UNCLASSIFIED.

5. P.J. Lamont and B.L. Hunt. "Pressure and Force Distributions on a Sharp-Nosed Circular Cylinder at Large Angles of Inclination to a Uniform, Subsonic Stream," *J. Fluid Mech.*, Vol. 76, Part 3 (1976).

6. ———. "Prediction of Aerodynamic Out-of-Plane Forces on Ogive-Nosed Circular Cylinders," *J. Spacecraft and Rockets*, Vol. 14, No. 1 (1977).

7. National Aeronautics and Space Administration. *Prediction of Static Aerodynamic Characteristics for Space - Shuttle - Like and Other Bodies at Angles of Attack From 0° to 180°*, by L.H. Jorgensen. Ames Research Laboratory, Sunnyvale, Calif., NASA, Jan 1973. (NASA TN-D-6996, publication UNCLASSIFIED.)

8. McDonnell Douglas Astronautics Co.-West. *Agile Configuration Development Test.* Huntington Beach, Calif., MDC, April 1974. (MDC G5IJ6, publication UNCLASSIFIED.)

9. ———. *Agile External Geometry Test.* Huntington Beach, Calif., MDC, June 1973. (MDC G4027, publication UNCLASSIFIED.)

10. F.D. Deffenbaugh and W.G. Koerner. "Asymmetric Vortex Wake Development on Missiles at High Angles of Attack", *J. Spacecraft and Rockets*, Vol. 14, No. 3 (March 1977).

11. U.S. Army Missile Research and Development Command. Summary of the 4th Meeting of the DOD/NASA High Angle of Attack Working Group, 16-17 Feb 1977. Huntsville, Ala., Redstone Arsenal, Feb 1977. (Internal Technical Note TDK-77-1, publication UNCLASSIFIED.)

12. National Aeronautics and Space Administration. *Experimental Aerodynamic Characteristics for a Cylindrical Body of Revolution With Various Noses at Angles of Attack From 0° to 58° and Mach Numbers from 0.6 to 2.0*, by L.H. Jorgensen and E.R. Nelson. Ames Research Laboratory, Sunnyvale, Calif., NASA, Dec 1974. (NASA TM X-3128, publication UNCLASSIFIED.)

13. E.L. Fleeman and R.C. Nelson. "Aerodynamic Forces and Moments on a Slender Body With a Jet Plume for Angles of Attack Up to 180°," presented at the 12th Aerospace Sciences Meeting, Washington, D.C., 30 Jan-1 Feb 1974. Paper UNCLASSIFIED.

14. Naval Postgraduate School. *Aerodynamic Characteristics of an Axisymmetric Body Undergoing a Uniform Pitching Motion*, by L.H. Smith and R.H. Nunn. Monterey, Calif., NPS, 1975 (NPS S9NN75021, publication UNCLASSIFIED.)

15. G.S. Pick. "Investigation of Side Forces on Ogive Cylinder Bodies at High Angles of Attack in the M = 0.5 to 1.1 Range," presented at the 4th Fluid and Plasma Dynamics Conference, Palo Alto, Calif., 21-23 June 1971. Paper UNCLASSIFIED.

16. McDonnell Douglas Astronautics Co.-West. *Agile Configuration Variables Wind Tunnel Test*, by M.M. Briggs. Huntington Beach, Calif., MDC, June 1972. (MDC G2991, publication UNCLASSIFIED.)

17. ———. *A Wind Tunnel Investigation of the Aerodynamic Characteristics of IVC Missile Configurations at Angles of Attack up to 90°*, by M.M. Briggs. Huntington Beach, Calif., MDC, Oct 1970. (MDC G0713, publication UNCLASSIFIED.)

Appendix A

COMPUTER PROGRAM FOR THE COMPUTATION OF TVC6 PITCHING MOMENT COEFFICIENT AND NORMAL FORCE COEFFICIENT

```
3914633*SRAAM(1).TVC6ARO
      1            COMPILER(DIAG=3)
      2      C***PROGRAM TVC6ARO***
      3      C***COMPUTES CN AND CM FOR TVC6 MISSILE***
      4      C**:DATA IS EXTRAPOLATED FROM AGILE WIND TUNNEL DATA**
      5      C**ESTIMATED BODY ALONE CN FOR TVC 6**
      6      C**DATA IS TABULATED FOR MACH#S .6,.8,.95,1.1,1.2,1.6,2.,3.*
      7      C**FOR ANGLES OF ATTACK 0TO90 IN 5 DEG INCREMENTS**
      8            DIMENSION CNB(19,8),BMACH(8)
      9            DATA BMACH/.6,.8,.95,1.1,1.2,1.6,2.,3./
     10            DATA (CNB(I,1),I=1,19)/
     11           A0.,.22,.74,1.36,2.46,4.06,
     12           B6.09,8.49,11.,13.22,15.1,16.5,
     13           C16.8,20.4,23.1,24.9,26.2,27.1,26.9/
     14            DATA (CNB(I,2),I=1,19)/
     15           A 0.,.33,.85,1.74,3.04,4.89,
     16           B 6.93,9.21,11.6,14.3,17.2,20.1,
     17           C 22.7,25.4,26.9,28.4,28.9,29.1,29.4/
     18            DATA (CNB(I,3),I=1,19)/
     19           A 0.,.32,.87,1.69,3.76,5.11,
     20           B 7.52,10.3,13.2,16.2,19.3,22.3,
     21           C 24.3,25.8,27.1,28.2,29.4,30.3,31.3/
     22            DATA (CNB(I,4),I=1,19)/
     23           A 0.,.32,.89,1.87,3.46,5.73,
     24           B 9.07,12.8,16.6,20.5,24.3,27.5,
     25           C 29.9,31.9,33.5,35.3,37.6,39.,39.2/
     26            DATA (CNB(I,5),I=1,19)/
     27           A 0.,.24,.79,1.29,3.54,6.16,
     28           B 9.45,13.1,16.9,20.4,23.6,26.4,
     29           C 28.8,31.,33.4,35.6,37.4,38.4,38.5/
     30            DATA (CNB(I,6),I=1,19)/
     31           A 0.,.39,.95,2.31,4.66,7.76,
     32           B 11.23,14.8,17.7,20.5,23.2,25.8,
     33           C 28.6,31.1,33.,34.2,35.3,36.,36.4/
     34            DATA (CNB(I,7),I=1,19)/
     35           A 0.,.24,.99,2.66,5.01,7.89,
     36           B 10.7,13.3,16.,18.6,21.3,23.8,
     37           C 26.3,28.6,30.5,32.,33.2,33.9,34.3/
     38            DATA (CNB(I,8),I=1,19)/
     39           A 0.,.36,1.29,3.,5.17,7.34,
     40           B 9.63,12.2,14.6,17.1,19.5,22.,
     41           C 24.3,26.4,28.3,29.9,30.,30.,30./
     42      C*****************
     43      C**INPUT BODY ALONE CP/L ESTIMATE FROM ALPHA=0TO 180. (5DEG INCR)
     44            DIMENSION XCP(37)
     45            DATA XCP/2.5,25.,32.3,36.,38.5,41.,42.5,44.,
     46           A 44.5,45.,45.,45.,45.,45.,46.,47.5,48.,49.,49.5,
     47           B 50.,50.,51.,52.,52.5,54.,55.,55.,55.,55.,
     48           C 55.,56.,57.5,59.,61.5,65.,71.,81.5,100./
     49      C**DATA FOR FIN EFFECTIVENESS FOR C62F CONFIGURATION**
     50      C**MACH NOS OF .8,1.1,1.6,2.***
     51            DIMENSION FMACH(4),DCNF(19,4)
     52            DATA FMACH/.8,1.1,1.6,2./
     53            DATA (DCNF(I,1),I=1,19)/
     54           A 0.,.1,.35,.5,.8,1.1,1.3,
     55           B 1.5,1.4,1.4,1.3,1.2,1.1,
     56           C .9,.9,.6,.5,.8,.7/
```

```
      DATA (DCNF(I,2),I=1,19)/
     A 0.,.15,.4,.5,.8,1.,1.,1.2,
     B 1.4,1.2,1.1,1.,1.,1.2,1.4,
     C 1.3,1.4,1.3,.9,.8,1./
      DATA (DCNF(I,3),I=1,19)/
     A 0.,.15,.45,.6,.6,.7,.9,
     B .9,1.,1.,1.,1.,1.,1.,
     C 1.,.9,1.,.9,.8,1./
      DATA (DCNF(I,4),I=1,19)/
     A 0.,.1,.35,.45,.5,.65,.85,1.05,11*1./
C**DATA FOR FIN EFFECTIVE CP**
C**FOR REGIONS WITH MISSING DATA A VALUE OF X/CR=.5 IS USED**
      DIMENSION XCPF(19,4)
      DATA (XCPF(I,1),I=1,19)/
     A 6.52,6.52,1.48,2.39,1.52,1.13,.42,
     B -.19,.81,1.19,1.76,1.97,1.13,
     C 2.6,1.27,2.08,5.32,1.19,1.1/
      DATA (XCPF(I,2),I=1,19)/
     A 1.86,1.86,.19,2.39,1.02,.65,.97,
     B .43,.64,.16,-.14,.08,-1.09
     C -.91,-.81,.32,1.41,1.36,1.19/
      DATA (XCPF(I,3),I=1,19)/
     A 1.42,1.42,-.81,.52,2.52,1.57,.08,
     B 1.69,.13,.66,.65,1.13,-.2,
     C .52,1.41,.39,.96,1.19,1.86/
      DATA (XCPF(I,4),I=1,19)/
     A 5.2,5.2,.91,2.,.66,.32,-.42,
     B -.81,11*.5/
      DIMENSION MACH(20),CNTAB(37,11),CMTAB(37,11)
      REAL MACH
      DATA JM/1/,JM1/1/
C*************************************************************
      WRITE(6,100)
100   FORMAT(1X,'HOW MANY MACH #S?')
      READ(5,101)NMACH
101   FORMAT()
      WRITE(6,102)
102   FORMAT(1X,'INPUT MACH#S')
      READ(5,101)(MACH(I),I=1,NMACH)
      WRITE(6,103)
103   FORMAT(1X,'WHAT IS MAX. ALPHA?')
      READ(5,101)ALFMAX
      WRITE(6,104)
104   FORMAT(1X,'INPUT MOMENT REF. FIN LEADING EDGE AND CENTER FO GRAVITY
     A LOCATION IN INCHES FROM NOSE')
      READ(5,101)XREF,XFLE,XCG
      DIA=6.
      ALPHA=0.
      CR=4.5
      XL=120.
      DO 1 I=1,NMACH
      ALPHA=0.
      DO 2 J=1,37
C**INTERPOLATE WITH RESPECT TO MACH NO**
C**DETERMINE BODY ALONE CN***
      XM=MACH(I)
      IF(MACH(I).LT..6)XM=.6
```

```
      IF(MACH(I).GT.3.)XM=3.
      CALL VLOOK(XM,8,BMACH,JM,IM)
      JJ=J
      IF(J.GT.19)JJ=38-J
      DEL=(XM-BMACH(IM-1))/(BMACH(IM)-BMACH(IM-1))
      CN1=CNB(JJ,IM-1)+DEL*(CNB(JJ,IM)-CNB(JJ,IM-1))
      XM=MACH(I)
      IF(XM.LT..8)XM=.8
      IF(XM.GT.2.)XM=2.
      CALL VLOOK(XM,4,FMACH,JM1,IM1)
106   FORMAT(2I3)
      DEL=(XM-FMACH(IM1-1))/(FMACH(IM1)-FMACH(IM1-1))
      DCNF1=DCNF(JJ,IM1-1)+DEL*(DCNF(JJ,IM1)-DCNF(JJ,IM1-1))
      CPFN=XCPF(JJ,IM1-1)+DEL*(XCPF(JJ,IM1)-XCPF(JJ,IM1-1))
C**COMPUTE FIN CP DISTANCE FROM NOSE**
      XFIN=XFLE+CPFN*CR
      CMB=CN1*(XREF-XCP(J)*.01*XL)/DIA
      CMF=DCNF1*(XFIN-XREF)/DIA
      CM=CMB-CMF
      CN=CN1+DCNF1
C**COMPUTE STATIC STABILITY MARGIN**
      XX=XCG-XREF
      XBAR=-CM/CN-XX/DIA
C     WRITE(6,105)MACH(I),ALPHA,CN,CM,CMB,CMF,XBAR
      CNTAB(J,I)=CN
      CMTAB(J,I)=CM
105   FORMAT(1X,10(F8.2,1X))
      ALPHA=ALPHA+5.
      IF(ALPHA.GT.ALFMAX) GO TO 1
2     CONTINUE
1     CONTINUE
3     CONTINUE
      WRITE(6,110)
110   FORMAT(1X,'*******CN******')
      WRITE(6,107)
107   FORMAT(1X,'ALPHA ',30X,'MACH #')
      WRITE(6,108)(MACH(I),I=1,NMACH)
108   FORMAT(7X,11(F6.2,1X))
      ALPHA=0.
      DO 4 I=1,37,2
C     WRITE(6,109)ALPHA,(CNTAB(I,J),J=1,11)
      WRITE(14,199)(CNTAB(I,J),J=1,11)
4     ALPHA=ALPHA+5.
      WRITE(6,111)
111   FORMAT(1X,'********CM******')
      WRITE(6,107)
      ALPHA=0.
      DO 5 I=1,37,2
C     WRITE(6,109)ALPHA,(CMTAB(I,J),J=1,11)
      WRITE(13,199)(CMTAB(I,J),J=1,11)
199   FORMAT(12F6.2)
109   FORMAT(1X,12(F6.2,1X))
5     ALPHA=ALPHA+5.
      STOP
      SUBROUTINE VLOOK(VAR,LNTH,ARRAY,JLST,INDEX)
      DIMENSION ARRAY(LNTH)
      LOGICAL L1,L2
```

```
      20    L1=VAR.GE.ARRAY(JLST)
            L2=VAR.LE.ARRAY(JLST+1)
            IF(L1.AND.L2)GO TO 30
            IF(.NOT.L1)JLST=JLST-1
            IF(L1)JLST=JLST+1
            IF(JLST.GT.0.AND.JLST.LT.LNTH)GO TO 20
            WRITE(6,100)
     100    FORMAT(1X,'VARIABLE OUTSIDE ALLOWABLE LIMITS')
            RETURN
      30    INDEX=JLST+1
            END

@BRKPT PRINT$
```

Appendix B

COMPUTER PROGRAM FOR THE COMPUTATION OF OUT-OF-PLANE FORCES AND MOMENTS

57

```
3914933*SRAAM(1),YAWS
      1       C**PROGRAM YAWS**
      2       C ***COMPUTSE OUT OF PLANE FORCES AND MOMENTS ON OGIVE-
      3       C****CYLINERS USING METHODS OF LAMONT AND HUNT() SPACECRAFT
      4       C****V 14,NO.1,JAN.,1977)
      5             REAL L,LREF,MACH,MU
      6             DATA RTD/57.2958/,PI/3.14159267
      7             DIMENSION TA(51),CF(51)
      8             DIMENSION VS(11),RH(11),TMU(11)
      9             DATA VS/1117.,1098.,1078.,1058.,1037.,1017.,
     10            *995.,973.,971.,971.,971./
     11             DATA RH/.002378,.002049,.001756,.001497,.001267,
     12            *.001066,.00089,.000737,.0005857,.00046,.0003627
     13             DATA TMU/3.719,3.618,3.515,3.411,3.305,3.196,
     14            *3.086,2.974,2.961,2.961,2.961/
     15             R=5
     16             WRITE(6,108)
     17       108   FORMAT(1X,'INPUT FN,L,LREF,MACH,ALT,DIA')
     18             READ(5,100)FN,L,LREF,MACH,ALT,DIA
     19             ALPHA=10.
     20       C     WRITE(6,109)
     21             DO 13 JJ=1,37
     22       109   FORMAT(1X,'INPUT ALPHA')
     23       C     READ(5,100)ALPHA
     24       100   FORMAT()
     25       C***COMPUTE REYNOLDS #**
     26             RALT=ALT/5.+1.
     27             IALT=RALT
     28             DIFF=RALT-IALT
     29             VSND=VS(IALT)+DIFF*(VS(IALT+1)-VS(IALT))
     30             RHO=RH(IALT)+DIFF*(RH(IALT+1)-RH(IALT))
     31             MU=TMU(IALT)-DIFF*(TMU(IALT+1)-TMU(IALT))
     32             V=MACH*VSND
     33             DIA=DIA/12.
     34             REYD=RHO*V*DIA/MU
     35             REYD=REYD*1.0E07
     36             ALP=ALPHA/RTD
     37             TA=3.+.05*ALPHA
     38             FAC=7.-FN
     39             IF(TA.GT.FAC)TA=FAC
     40             TC=11.47+4.7*TAN(ALP)
     41             FAC=21.-2.*FN
     42             IF(TC.GT.FAC)TC=FAC
     43             IF(REYD.LT.200000.)GO TO 16
     44             TA=1.+.05*ALPHA
     45             FAC=5.-FN
     46             IF(TA.GT.FAC)TA=FAC
     47             TC=9.47+4.7*TAN(ALP)
     48             FAC=19.-2.*FN
     49             IF(TC.GT.FAC)TC=FAC
     50       16    CONTINUE
     51             TB=(.6+.1*COS(2.*ALP))*(TC-TA)+TA
     52             TE=TC-4.+2.6*TAN(ALP)
     53             TG=TE+4+2.6*TAN(ALP)
     54             CBMX=1.+.4*FN
     55             XM=0.6-TA
     56             XC=TC-TA
```

```
      X=4.6*FN*TAN(ALP)-TA
      IF(X.GE.0.)GO TO 1
      CB=1.
      GO TO 3
1     IF(X.GE.XC)GO TO 2
      IF(X.GT.XM)GO TO 17
      CB=1.+(CBMX-1.)*X/XM
      GO TO 3
17    CB=CBMX-CBMX*(X-XM)/(XC-XM)
      GO TO 3
2     CB=0.
3     CONTINUE
      IF(REYD.GE.200000.)CB=CB*.8
      IF(MACH.LT..6)FMACH=1.
      IF(MACH.GE..6)FMACH=1.-(MACH-.6)
      IF(MACH.GT.1.6)FMACH=0.
      CB=CB*FMACH
C**COMPUTE OUT OF PLANE FORCE DISTRIBUTION**
      TMAX=L*TAN(ALP)/R
      H=TMAX/50.
      T=0.
      DO 4 I=1,51
      TJ(I)=T
      IF(T.GT.TA)GO TO 5
      CF(I)=0.
      GO TO 9
5     IF(T.GT.TC)GO TO 6
      X=PI*(T-TA)/(TC-TA)
      XB=PI*(TB-TA)/(TC-TA)
      CF(I)=CB*EXP((XB-X)/TAN(XB))*SIN(X)/SIN(XB)
      GO TO 9
6     IF (T.GT.TE)GO TO 7
      XI1=(T-TC)*PI/(TE-TC)
      CF(I)=-.6*CB*SIN(XI1)
      GO TO 9
7     IF(T.GT.TG)GO  TO 8
      XI2=PI*(T-TE)/(TG-TE)
      CF(I)=.3*CB*SIN(XI2)
      GO TO 9
8     CF(I)=0.
9     CONTINUE
      T=T+H
4     CONTINUE
C**COMPUTE SIDE FORCR USING SIMPSONS RULE FOR INTEG**
      SUM=0.
      DO 10 I=2,50
10    SUM=SUM+CF(I)
      XINT=.5*H*(CF(1)+2.*SUM+CF(51))
      CY=2.*SIN(ALP)*COS(ALP)*XINT/PI
C***COMPUTE MOMET COEFF.**
      TREF=LREF*TAN(ALP)/R
      SUM=0.
      DO 11 I=2,50
11    SUM=SUM+(TREF-TJ(I))*CF(I)
      XINT=.5*H*(TREF*CF(1)+2.*SUM+(TREF-TMAX)*CF(51))
      CETA=((COS(ALP))**2)*XINT/PI
      DIA=DIA*12.
```

```
      WRITE(,101)ALPHA,FN,L,LREF,DIA,MACH,ALT,REYD
101   FORMAT(1X,'ALPHA=',F6.2,'FN=',F6.2,'LENGTH=',F6.2,
     * 'REF LENGTH=',F6.2,'DIAM=',F6.2,'MACH#=',F6.2,
     * 'ALT(KFT)=',F6.2,'REYD=',E10.2)
      WRITE(6,102)TA,TB,TC,TE,TG,TMAX,TREF
103   FORMAT(1X,'A1=',E12.6,'A2=',E12.6,'A3=',E12.6)
C     WRITE(6,104)
104   FORMAT(1X,'X/R',2X,'T',9X,'CF')
C     DO 12 I=1,S1
C     XR=TJ(I)/TAN(ALP)
C     WRITE(6,105)XR,TJ(I),CF(I)
105   FORMAT(1X,F5.2,1X,F7.3,1X,F7.3)
12    CONTINUE
      WRITE(6,106)CY,CETA
      WRITE(6,107)
107   FORMAT(1H )
13    ALPHA=ALPHA*2.
15    CONTINUE
14    CONTINUE
106   FORMAT(1X,'CY=',F6.2,'CETA=',F6.2)
102   FORMAT(1X,'TA=',F6.2,'TB=',F6.2,'TC=',F6.2,'TE=',F6.2,
     * 'TG=',F6.2,'TMAX=',F6.2,'TREF=',F6.2)
      STOP
      END
```

@HDG,P NORMAL FORCE AND PITCHING MOMENT COEFFICIENTS

@PRT,S S.TVC6ARO
FUPPUR 27R1 RL72-8 12/28/77 13:37:30